EFFECT OF FLUXES ON CRACKING DURING ESS OF STEEL WITH 70/30 CUPRONICKEL STRIP

Jingying Zhang

B.S., Shanghai Jiao Tong University, Shanghai, China, 1988

A thesis submitted to the faculty of the

Oregon Graduate Institute of Science & Technology

in partial fulfillment of the

requirement for the degree

Master of Science

in

Materials Science and Engineering

July, 1994

The thesis "Effect of Fluxes on Cracking During ESS of Steel with 70/30 Cupronickel Strip" by Jingying Zhang has been examined and approved by the following Examination Committee:

Jack H. Devletian, Thesis Advisor
Professor

Jim Stanley
Assistant Professor

Milt Scholl
Assistant Professor

To My Parents

ACKNOWLEDGEMENTS

TABLE OF CONTENTS

LIST OF TABLES

LIST OF FIGURES

ABSTRACT

Effect of Flux Composition on Cracking during ESS of Steel with 70/30 Cupronickel Strip

Jingying Zhang, M. S.
Oregon Graduate Institute of Science & Technology, 1994

Supervising Professor: Jack H. Devletian

The effect of flux composition on the weldability of multi-layer cladding deposited on steel with 70/30 cupronickel strip electrodes by the electroslag surfacing (ESS) process was investigated. For comparison purpose, two nearly similar commercial fluxes were used: Flux 1 caused severe solidification cracking and ductility-dip cracking while Flux 2 resulted in extremely crack-resistant cladding. The objective of this study was to determine the mechanism of cracking in this cladding system.

The mechanism of cracking was found to be caused by the segregation of interdendritic Ti and other low melting constituents. The segregation of impurities resulted in the lowering of the liquidus and solidus temperatures of the cupronickel alloy, and was responsible for cracking. When a beneficial element Ce (in the form CeF_3) was added to the Flux 1, the cracking in cupronickel cladding deposited on MIL-S-23284, Class 1 steel with a buttering layer of 70Ni-30Cu was efficiently prevented. The prevention of cracking was associated with the slag-metal reaction taking place in the molten pool during the ESS process. The addition of Ce was introduced from the flux to react with Ti and other detrimental elements, such as S, P, O, and Mg, to form innocuous complex Ce-containing compounds. In cladding 2 deposited with flux 2 (containing 5-15% CeF_3), innocuous inclusions rather than trace alloying elements were generated. As a result, the Ce provided a means to significantly eliminate cracking by mitigate the effect of detrimental trace elements responsible for solidification cracking and ductility-dip cracking.

xi

CHAPTER 1
INTRODUCTION

Copper-nickel alloys are well known for their resistance to corrosion, erosion and the destructive effects of sea water. For over forty years the United States Navy has made extensive use of 70/30 cupronickel. The large applications continue to be for condenser tubes and ships' propellers. The last 10 to 20 years have seen major new marine application areas for copper develop in the offshore oil and gas industry and in desalination plants producing fresh water from the sea.[1-4]

Although there have been a number of investigations into the weldability of the 70/30 cupronickel alloys, weld cracking in its various forms still remains a problem. From previous investigations it is evident that cracking can take the form of solidification cracking in the weld metal,[5-11] liquation cracking in the heat affected zone[6,8] and ductility dip cracking in the heat affected zone.[5,9-11] For hot cracking, the fundamental mechanisms are generally understood. Both metallurgical and mechanical factors are present to cause hot cracking. The nature of the temperature distribution and the comparatively rapid temperature change associated with welding make the existence of complex stresses unavoidable. Thus, appropriate changes in welding procedure may minimize the stresses and associated strains. In the other hand, the occurrence of hot cracking requires consideration of the effect of microsegregation produced during solidification. In general, the subgrain and grain boundaries produced during solidification become enriched with solute species which tend to lower the effective melting temperature of the alloy. The resulting solute-rich subgrain and grain boundaries constitute the major form of microsegregation present in weld metal and provide the most likely sites for nucleation and propagation of hot cracks by the strains associated with welding. Any alloying process which reduces the effect of segregating impurities to a

1

minimum is obviously advantageous.

It is recognized that the choice of welding conditions influences the mechanics of solidification and therefore, the form and severity of the microsegregation. Therefore, hot cracks can be eliminated by choosing the proper welding conditions. In this research, attention has been given to the fluxes which have significant influences on the weldability of 70/30 cupronickel alloy during ESS process. The results of this study indicated that beneficial elements could be introduced to the cladding from flux during welding which would reduce the segregation of impurities. The objectives of this study were :

(1) To study the microstructural changes with different fluxes,

(2) To evaluate the effect of trace elements such as Ti, Ce, Fe, Al, Si, Mg, S, P, and O on the hot-cracking behavior of cupronickel weld metal, and

(3) To investigate the mechanism of hot cracking in cupronickel cladding

CHAPTER 2
BACKGROUND

2.1 70/30 CUPRONICKEL ALLOY:

70/30 Cupronickel is basically a single phase alloy. With small additions of iron and manganese, it offers outstanding seawater corrosion and biofouling resistance.[6] One important application of this alloy is used for the surface protection of carbon steel. However, hot cracking is a common welding problem which often occurs in this alloy. Both weld metal cracking and heat affected zone cracking were observed by previous researchers.[5-11] The effect of trace impurities on hot cracking of cupronickel alloys has been studied by some researchers. A review of the previous work will now be made in the following text.

Iron

Iron addition is made to cupronickel alloys to improve the resistance to corrosion, particularly under impingement conditions.[7] It is generally considered an innocuous alloying addition having little effect on either the mechanical properties or weldability at low concentrations in Cu-Ni alloys.[7,8] However, adding increasing amounts of iron to the 90/10 cupronickel alloy was reported to reduce the ductility of the alloy in the intermediate temperature range. Billingham et al[12] indicated that the level of iron in the alloy should be kept to 1% or below to ensure adequate intermediate temperature ductility. Wilson and his co-workers[55] studied the effect of iron dilution on cupronickel weld deposits and indicated that 16%wt iron was the maximum level for 70/30 cupronickel alloy to avoid cracking, 11.8%wt iron was the maximum level for 70/30 cupronickel alloy to avoid losing corrosion resistance.

3

Manganese

Manganese is added to cupronickel alloys to aid melt fluidity, to counteract the harmful effect of sulfur impurities, and has also been reported to both strengthen and improve weldability if added in sufficient quantity.[12] Billingham et al[12] reported that manganese could be added up to 5% level to aid melt fluidity if required without seriously impairing ductility. However, a deleterious effect of manganese was reported by Savage et al[8] that in the presence of Mn, the combination of Fe and Sb was detrimental. This was associated with segregation of manganese to the grain boundary regions which resulted in a lowering of the melting point of the boundary.

Silicon

Silicon is added to cupronickel alloys to provide strengthening by means of precipitation reactions. This element, however, has a markedly deleterious effect on intermediate temperature ductility. It was reported by Billingham et al[12] that a pronounced ductility trough occurred as Si was increased to 0.5%wt. Si was also reported to be a weld metal crack promoter by Petersen[7] when above 0.6%wt and by Jordan[13] at the level of 1%.

Aluminum

Aluminum is added to cupronickel alloys to play the same role as silicon. Although it was reported to be a detrimental element, it has much higher tolerable amount than that of Si. Billingham et al[7] reported that small additions of aluminum (0.1%) gave acceptable ductility. As Al increased beyond 5%wt, the intermediate temperature ductility was decreased.

Titanium

Titanium is added to cupronickel alloys as a deoxidant. It was reported by Petersen[7] that the quantity of Ti greater than that required for deoxidation (about 0.1%) did not offer any beneficial effect on weldability. Ti increased cracking when acting

singly in the absence of other impurities. Pease and Kihlgen[14] indicated that Ti levels > 0.15%wt could cause weld metal cracking. This was associated with formation of low freezing point eutectics which persisted in the interdendritic regions and thereby caused cracking during solidification. Jordan and Duncan[13] proposed that when other impurities were present, i.e. P with Ti, the crack inhibiting interaction occurred. This could be due to a combination between the elements. Such a combination could reduce the level of the element in solution and thereby reduce the extent of cracking.

Phosphorus

Phosphorus is universally identified as an embrittling element in cupronickel alloys subjected to hot work. It has been reported that phosphorus is also injurious to the weldability of the cupronickels. When present in oxygen-free Cu, P results in a loss of high-temperature ductility. In 70/30 cupronickel, Lee et al[5] showed that cracking increased with increasing phosphorus (30 to 300 ppm). A study of the 70/30 cupronickel alloy made by Savage et al[8] indicated that the cracking increased as phosphorus increased from 8 to 60 ppm. A detrimental interaction of P and Fe was also reported in his study. The needle-like phosphorus-rich precipitates were observed by Billingham et al[15] along the grain boundaries of the alloy. Such precipitates could act as stress risers and encourage premature intergranular cracking behavior, thereby increase the tendency of the alloy to mid-temperature brittleness. The effect of P in promoting cracking has been attributed both to the formation of low melting point liquid films and to the presence of P enriched solid films.

Sulphur

Sulphur was reported to be a cracking promoter in cupronickel alloys. Jordan and Duncan[13] reported that S content of 0.02%wt or greater increased cracking susceptibility. Billingham et al[15] indicated that the safe limit of sulphur was up to 750 ppm wt. Sulphur was also reported to segregate to the region of the cracks. It was proposed that the mechanism of the S effect was similar to that of P, i.e. the forming of

low freezing point liquid films and brittle solid films during solidification and subsequent cooling.

Oxygen

In welding of cupronickel alloys, the presence of oxygen is inevitable. According to Lancaster,[53] a steam reaction may occur when hydrogen and oxygen are simultaneously present in the liquid metal or in the solid at elevated temperature. The reaction can be represented by:

$$Cu_2O + H_2 = 2Cu + H_2O$$
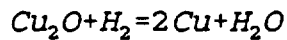
The steam reaction is responsible for the porosity to which fusion welds in cupronickel are subject. Kobayashi et al[58] studied the effect of oxygen content of argon-oxygen mixtures at total pressure of 1 atm on porosity of GMA welds in copper, and indicated that up to a partial pressure of 0.1 atm, oxygen reduced the amount of porosity; above this level the porosity increased again. In addition to the porosity, the oxygen was reported by Lebedev et al[56] to form a Cu-Cu$_2$O eutectic on the grain boundaries at copper base alloy. This eutectic was responsible for the intergranular embrittlement and the decrease in ductility of this alloy.

Other Elements

Chromium was reported to be a cracking promoter by Petersen.[7] The threshold figure for cracking in his study was 3.75%wt. In 90/10 cupronickel, Witherall[6] specified the crack free levels of Bi < 80 ppm, Cd < 200 ppm, P < 200 ppm, Pb < 200 ppm, Se < 300 ppm and Te < 200 ppm. In 70/30 alloy he specified the optimum crack free levels of P < 200 ppm, Pb < 500 ppm and Te < 200 ppm. Billingham and his associates[15] found that increasing the levels of the impurities Bi, Pb, Se, S and Te over the range 1-750 ppm wt brought a severe reduction in the intermediate temperature ductility. The safe limits of these elements were Bi < 20 ppm, Te < 45 ppm, Pb < 120 ppm, Se < 150 ppm and S < 750 ppm. In their study, a Bismuth Equivalent

formula based on the effect of Bismuth on the ductility trough behavior was carried out:

$$BiE = Bi + 0.7Te + 0.4Pb + 0.2Se + 0.1S$$

2.2 ELECTROSLAG SURFACING (ESS) PROCESS:

Cupronickel alloys can be joined by most of the commonly used processes,[16-21] such as oxyacetylene welding, shielded metal-arc welding, submerged arc welding, gas tungsten-arc welding, gas metal-arc welding, resistance and induction welding. Of these processes, gas tungsten-arc welding and gas metal-arc welding are the most popular processes. Recently, the electroslag surfacing process has been adapted to clad steel with cupronickel alloy.

Electroslag surfacing (ESS) has long been recognized as the most cost-effective method to surface thick-section (above 40 mm) steel and stainless steel plates.[22,23] Compared to other processes, ESS has many advantages including: high welding speed, less welder skill requirement, low dilution, low penetration, and high deposition rate.[24-28] As a welding process, it also produces high quality welds, since the slag pool protects the weld metal from the atmosphere.

The principle of the ESS process is shown in Figure 1. The ESS process uses the heat generated by resistance heating of the slag pool to melt and fuse the base and filler metals together. The molten metal as well as the molten slag pool are contained in the joint by the parts to be welded. The slag pool floats above the molten metal and provides shielding from the atmosphere. As filler metal is being fed into the weld pool, it sinks to the bottom due to its higher density. The weld metal solidifies progressively from the bottom upward.

2.3 SLAG-METAL REACTIONS IN THE ESS PROCESS:

During electroslag surfacing (ESS), as in other flux-shielded processes, chemical reactions take place between the slag and the metal. This interaction results in

compositional changes affecting the structure and properties of the weldment and hence is of considerable practical importance. Over the last three decades, the research of slag-metal reactions in welding has been developed by many investigators.[29-39] Mitra and Eagar[33-35] proposed a kinetic model to explain this interaction. In their report, it was proposed that chemical interactions between the slag and the metal occurred in three zones, as indicated in Figure 1:

(1) a zone of droplet reactions,

(2) a zone of dilution and weld pool reactions, and

(3) a zone of cooling and solidifying weld pool.

Zone of Droplet Reactions

In this region, the droplet forms at the electrode tip (Fig. 1). The entire process occurs in a few milliseconds, and the temperature of the droplets is very high. Due to the high temperature, it is thermodynamically possible for several chemical reactions to occur. The alloying elements Si, Mn, and Al are not transferred in this zone[33] while oxygen is.[31] In multiple-pass welds, the top weld pass contains more oxygen than the bottom layer.

Oxygen which is transferred to the metal in this zone has two possible sources:

(1) decomposition of flux constituents into suboxides and oxygen, and

(2) contamination from the atmosphere.

The decomposition of flux constituents into suboxides and oxygen appears to be the primary source of oxygen. Different fluxes will produce different oxygen levels in the weld metal depending on the stability of the flux constituents.[36-39] Contamination by oxygen from the atmosphere plays a much smaller role[36-38] but cannot be totally neglected as a source of oxygen.

Zone of Dilution and Weld Pool Reactions

In this zone, the falling droplets become "diluted" with molten metal from baseplate (Figure 1). The high temperature and the large convective forces in this region

Strip ⟶

(1) Droplet Reactions

(3) Cooling and Solidifying Weld Pool

Flux

Solidified Slag

Liquid Slag

Weld Deposit

Base Metal

Welding Direction

(2) Dilution and Weld Pool Reactions
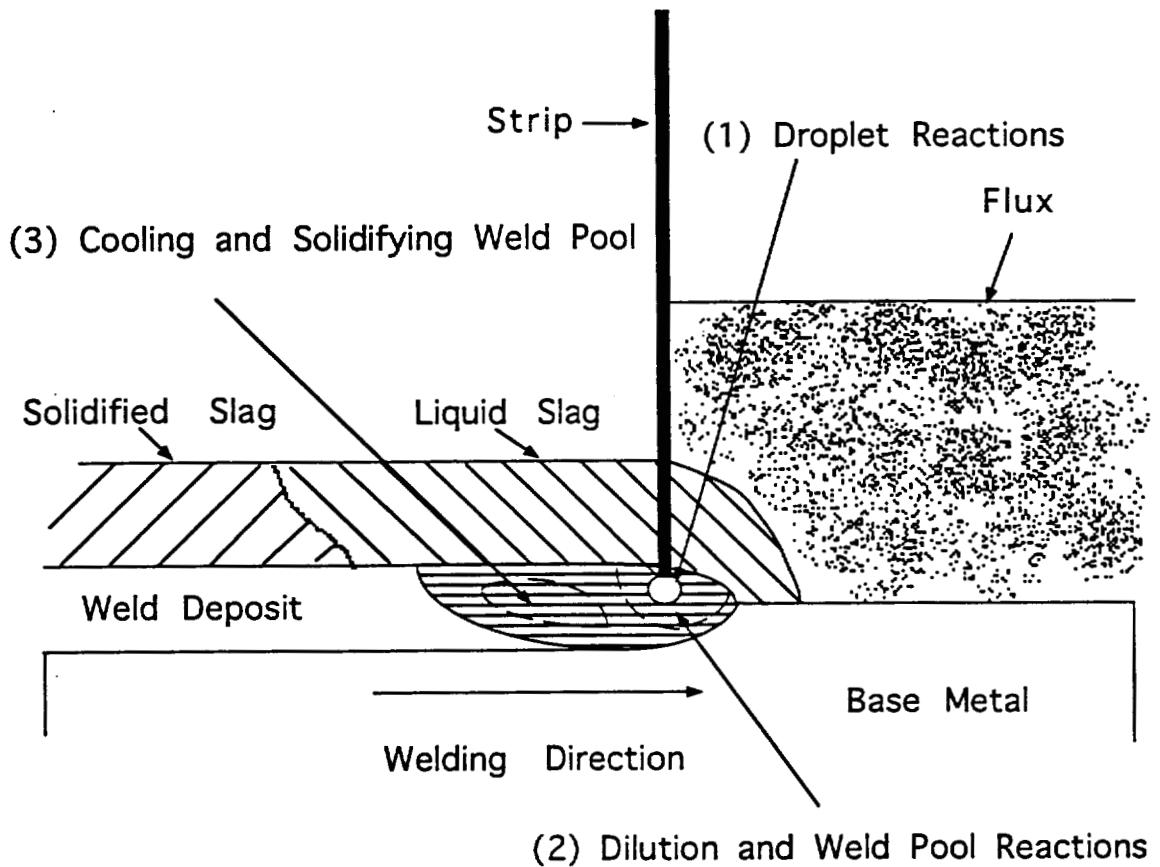
Figure 1. Electroslag Surfacing Process and The Three Reaction Zones
(1) A zone of droplet reactions
(2) A zone of dilution and weld pool reactions
(3) A zone of cooling and solidifying weld pool

lead to intimate mixing of the molten metal and result in vigorous chemical reactions at the slag-metal interface. It was proposed that the transfer of an alloying element M may occur by the reaction:

$$\underline{M} + x\underline{O} = (MO_x) \tag{1}$$
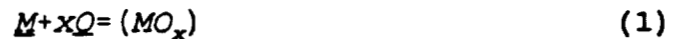
A kinetic model was formulated to predict weld metal composition.

For single-pass welds, the following equation was suggested:

$$M_f = NP - (NP - M_i) \cdot \exp(-\alpha (A_{s/m} / V_m)) \tag{2}$$

where M_f = the final alloy content of element M in the weld metal;

NP = the neutral point composition at which no metal transfer takes place;

M_i = the initial content of M in the weld metal;

α = a parameter which incorporates the mass transfer coefficient and the partition coefficient between slag and metal;

$A_{s/m}$ = the area of the slag-metal interface; and

V_m = the volume of the weld metal.

For multipass welds, when several passes are made without changing the welding consumables or process parameters, Eq. (2) leads to a steady-state value of metal composition.

$$M_N = M_{e_1} + \frac{(NP - M_{e_1})(1 - F)}{(1 - Fd)} \tag{3}$$

where M_N = the composition of the Nth weld Layer;

M_{el} = the electrode composition;

d = the dilution of the electrode with the baseplate; and

F = a parameter which incorporates the kinetic considerations including the effect of variations in the welding process parameters. It is

$$F = \exp(-\alpha (A_{s/m} / V_m)) \tag{4}$$

Zone of Cooling and Solidifying Weld Pool

In this region, the molten weld pool behind the electrode starts to cool and solidify as the electrode moves away from it. The increased stability of oxides at lower temperatures and the high amounts of oxygen present in the weld pool will result in the formation of inclusions or deoxidation products inside the molten metal. Furthermore, these inclusions may grow with time by coalescence, and the larger ones are more likely to separate from the liquid metal into the slag.[26-28] If the weld pool contains larger amounts of alloying elements, oxygen supersaturation and consequent inclusion formation will occur earlier, at higher temperatures. These inclusions will thus have more time to grow and separate.

It should be noted that the main factor controlling weld metal oxygen is flux composition. However, the welding parameters and the alloy content of the electrode and baseplate also significantly influence final weld metal oxygen content, due to a mechanism of inclusion formation and removal in the cooling weld pool. The effect of the welding parameters on weld metal oxygen is particularly significant on welding with highly oxidizing fluxes.

2.4 SOLIDIFICATION IN WELD METAL:

A weld zone may be considered as a continuous casting, formed under specialized conditions: an intensely stirred liquid pool, high temperature gradients, rapid growth rates, intimate contact between the molten alloy and the mold including partial melting of the mold. Weld solidification usually is presented as two steps: (1) initial solidification, and (2) crystal growth.

1. Initial Solidification

In weld metal solidification, the nucleation step is usually not required.[40] The molten alloy of the fusion zone freezes within a mold formed of the base metal. The alloy, as its heat of fusion is transferred to the base metal, may grow epitaxially on the

base metal. Each base metal grain at the fusion line may serve as the growth site for a fusion zone grain. Thus, the initial size of the grains at the fusion line will be the same as the grain size of the base metal at the fusion line at the time freezing begins at that location. Also, the crystallographic orientation of each fusion zone grain will be the same as the orientation of the base metal grain on which it grows epitaxially.

2. Crystal Growth and Segregation

As the weld metal continues to solidify, the grains that have a preferred crystallographic axis closely aligned with the heat flow direction quickly outgrow those grains with less favorable orientation. The growth of a favorably oriented crystal under the conditions expected of fusion welding, i.e. an initially high temperature gradient and good mixing in the liquid, is now discussed.[41] For the sake of simplicity the solidification of a binary alloy is considered, as shown in Figure 2. Since the cooling rate of fusion welds is high, weld solidification may not occur under equilibrium conditions. In the initial stages of solidification good mixing of the liquid seems likely due to the turbulence of the melt. However, as the heat source moves away and solidification goes to completion it seems likely that convectional mixing gives way to diffusional mixing. On this basis, two cases will be reviewed:

(1) No diffusion in solid; perfect mixing in liquid, and

(2) No diffusion in solid; diffusional mixing in liquid.

No diffusion in solid; perfect mixing in liquid

Consider a cylindrical volume element of the growing crystal, Figure 3. Referring to Figure 2, an alloy of composition X_0 has a liquidus temperature of T_1 . According to Flemings[41], a partitioning coefficient, k, is defined by Eq. (5).

$$k = \frac{X_S}{X_L}$$

(5)

Where X_S and X_L are the mole fractions of solute in the solid and liquid which coexist

with one another at a given temperature. Thus, at a temperature T_1 the first solid to form contains kX_0 of solute. Since $kX_0 < X_0$, this initial solid is purer than the liquid from which it forms. This implies that solute has to be rejected into the liquid, raising its concentration to above X_0. The next layer of solid will be richer in solute than the first. As this sequence of events continues the liquid becomes progressively richer in solute and solidification occurs at progressively lower temperatures. Since there is no diffusion in the solid, the separate layers of solid retain their original compositions so that the mean composition of the solid is continuously lower than the solidus composition given by the phase diagram, i.e. the true solidus is defined by X_S in Figure 2. On the other hand, the liquid becomes progressively richer in solute and may even attain eutectic composition at the temperature T_E. The corresponding composition profiles for the volume element will thus progress as shown in Figures 3(b) and (c).

No diffusion in solid; diffusional mixing in liquid

If there is no stirring or convection in the melt, the solute rejected into the liquid during solidification can only be transported away from the solid-liquid interface by diffusion. There will thus be a build-up of solute ahead of the growing crystal, with a corresponding rapid increase in alloying content of the solid that forms (Figure 4). The concentration profile in the liquid ahead of the interface is given by Eq. 6.

$$X_L = X_0\{1 - \frac{1-k}{k}\exp[-\frac{x}{D/R}]\} \qquad (6)$$

where $D =$ diffusivity of the melt

$\quad X_L =$ the solute concentration of the liquid

$\quad R =$ the growth speed of the crystal

$\quad x =$ the distance from the interface

This equation indicates that X_L decreases exponentially from X_0/k at $x = 0$ (the interface) to X_0 at some distance from the interface. As indicated by Figure 4, in the final stages of solidification, the "bow-wave" of solute is compressed into a comparatively small
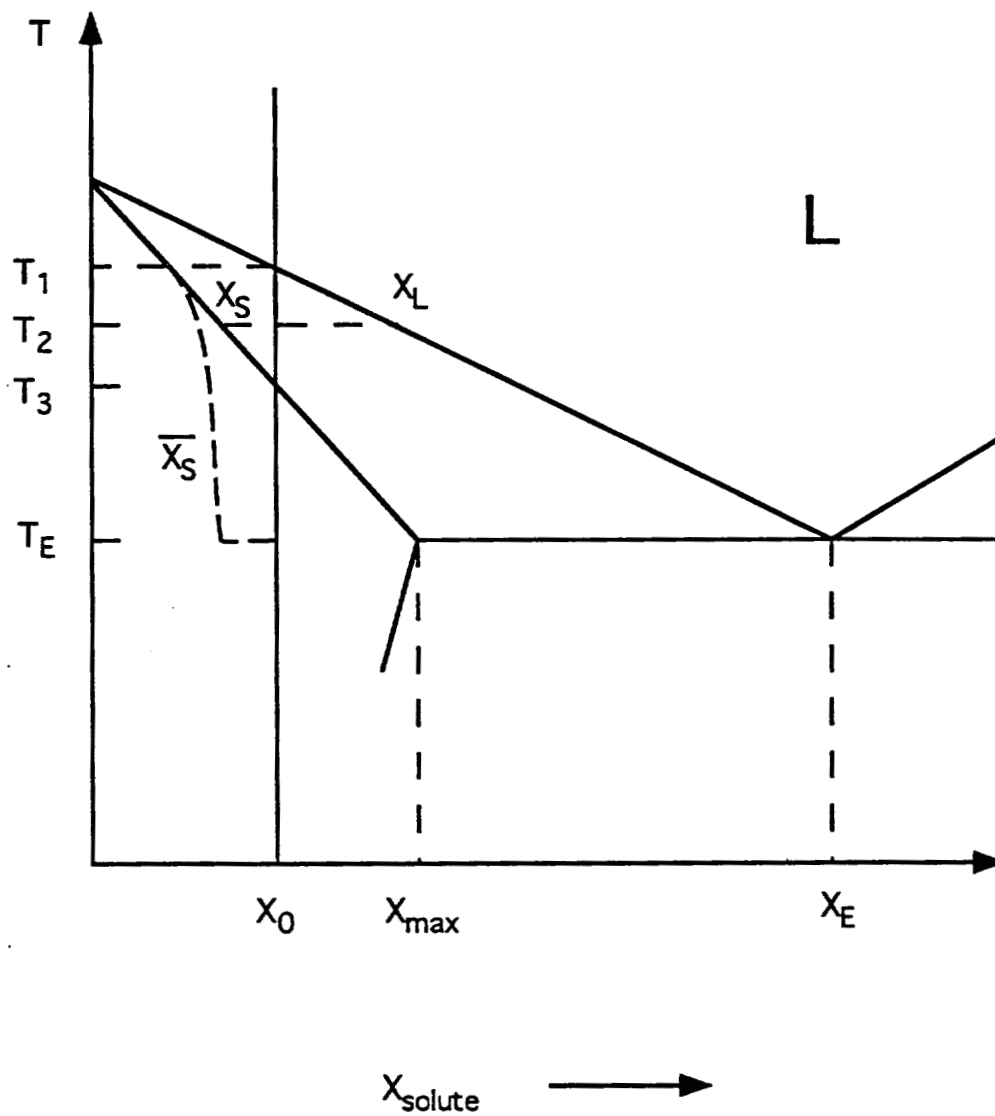
Figure 2. The non-equilibrium solidification of an alloy, X_0 in a simple binary system
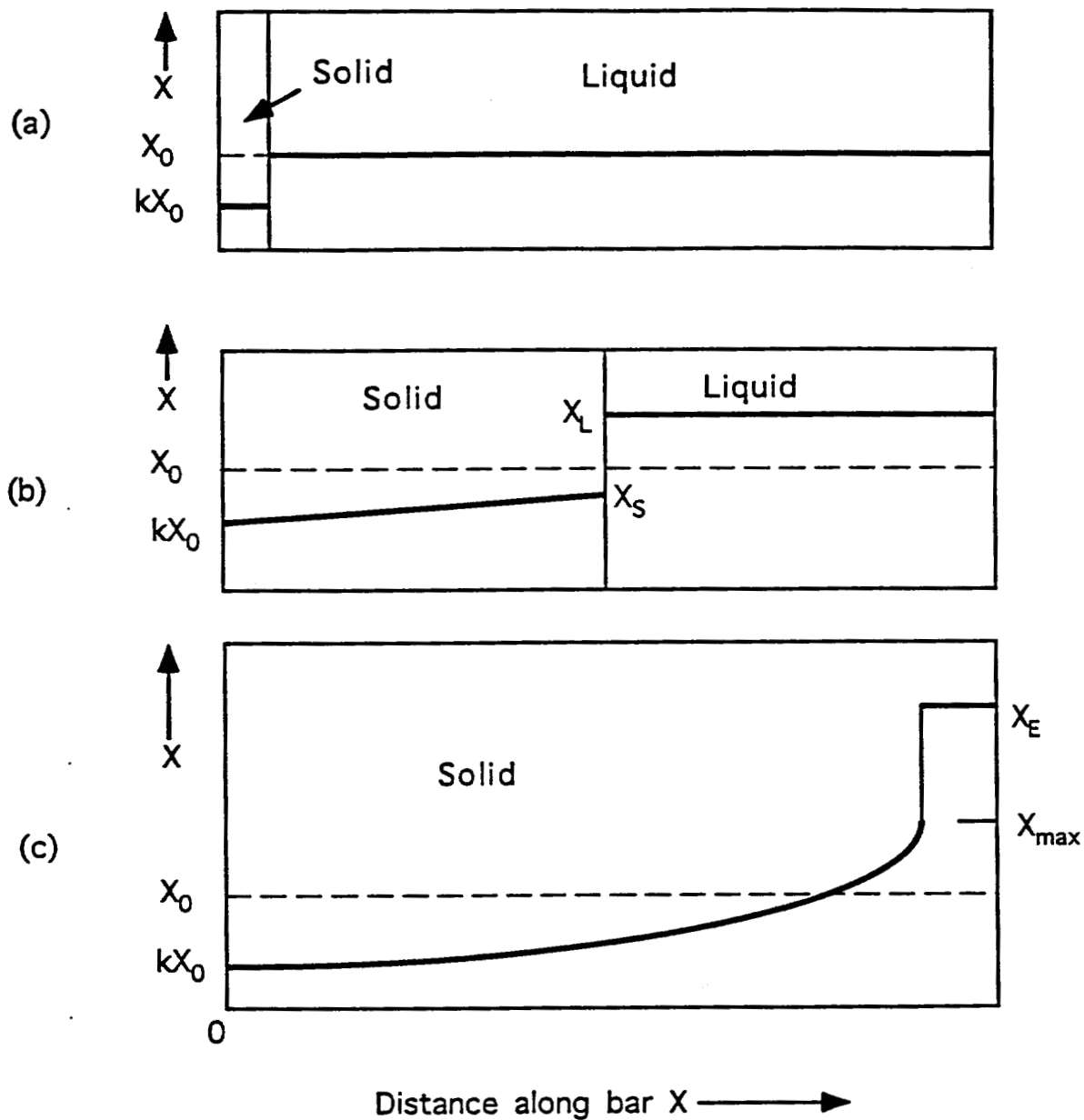
Figure 3. Solidification of a binary alloy when there is perfect mixing in the liquid and no diffusion in the solid. The composition profile in a solidifying cylindrical bar will progress as shown from (a) to (c).
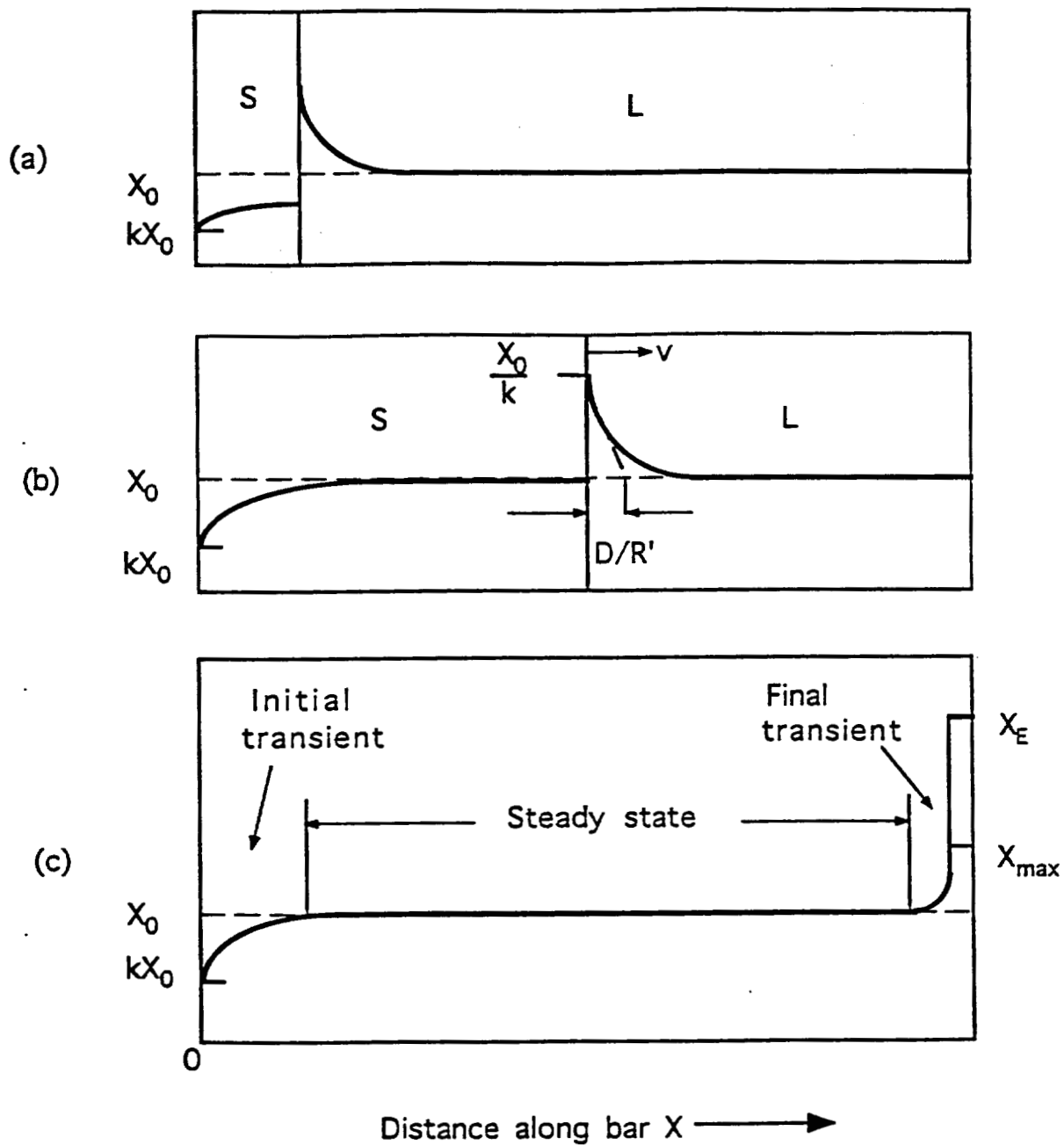
Figure 4. Solidification when mixing in the liquid is controlled by diffusion, the composition profile of a solidifying bar appears as the sequence (a) to (c).

volume of liquid and the solute composition is thus expected to rise rapidly. In terms of weld solidification, this suggests that the last stages of weld solidification are associated with the highest level of segregation.

A simple binary system is considered above, but most weld metals contain a number of impurities and alloying elements. As a general rule, alloying elements or impurities that tend to widen the solidification range, or that possess a low partition coefficient, k, will increase the amount of segregation.

2.5 HOT CRACKING IN WELD METAL:

Hot cracking (ie. solidification cracking and ductility-dip cracking) which occurs during welding is one of the serious problems in cupronickel alloys. During or immediately after solidification, when fusion welding is applied, most of the alloys will pass through a temperature range in which ductility is very low. Hot cracking occurs in these low ductility ranges when thermal tensile strains induced by internal contraction and external displacement exceed endurable strains. Hemsworth et al[42] classified hot cracking using behavior of ductility curve during and after solidification that "Segregation cracking" associated with microsegregation leading to intergranular films and "Ductility-dip cracking" occurring at newly migrated grain boundaries free from liquid films. In the solidification brittleness temperature range (BTR), "super-solidus cracking" tends to occur; that is, solidification cracking in weld metal and liquation cracking in multipass weld metal. In ductility-dip temperature range (DTR) after solidification, "sub-solidus cracking" or "ductility-dip cracking" tends to occur in primary weld metal or reheated (multipass) weld metal.

Super-solidus cracking is caused by separation of solidification grain boundaries along which residual liquid films or droplets are existing. Concerning the mechanism of solidification cracking in welds many theories have been proposed.[43-50] Of these theories the most reasonable one which provides the best understanding of the many observed phenomena of solidification cracking is known as the "Generalized Theory" and is

ascribed by Borland.[46,47] Borland has proposed four solidification stages as shown in Figure 5 with cracking susceptibility curve: Stage 1; no cracking occurs in this stage due to a large quantity of residual liquid. Stage 2; interlocking of dendrites starts but residual liquid is capable of relative movement between interlocking dendrites. No cracking occurs in this stage due to refilling and healing by interconnecting residual liquid. Stage 3; crack susceptible stage due to noncapable of healing by remaining liquid. The solid crystals are in an advanced state of development here and a semicontinuous network of solid restricts the free passage of remaining liquid. This is called the "critical solidification range". No healing of cracks is possible if accommodation strain is exceeded because the remaining liquid volumes are not interconnected. Stage 4; no cracking stage due to high tolerable strength in complete solidification. The temperature difference in the "critical solidification range" is considered to be in proportion to that of nominal liquidus and solidus temperature in general. Welds do not solidify under equilibrium conditions, so that the nominal solidus will be depressed by coring and lack of time for diffusion. In multicomponent systems with impurities, the true solidus can be severely depressed. This leads to a wider temperature range during stage 3 for restraint to build up and severe cracking may occur.

Weld metal solidification cracking of cupronickel alloys has been found by many investigators. Witherell[6] observed the fusion line cracking in the cupronickel weld metal which was welded by gas metal-arc process. Savage and his co-workers [8-10] used a Tigamajig test to resemble the multiple-pass weld of 70/30 cupronickel alloy made under restraint, and the hot cracking was observed in the weld metal.

Sub-solidus cracking is considered to be caused by separation of migrated grain boundaries after solidification is completed. This cracking usually occurs at boundaries which are free from films, and it is usually accompanied by a ductility trough. Segregation, precipitation or sliding of the migrated grain boundaries are reported to be related to cause cracking.[51]

Ductility-dip cracking is another type of hot cracking which often takes place in cupronickel alloys. Lee et al[5] observed the ductility-dip cracking when sulphur was
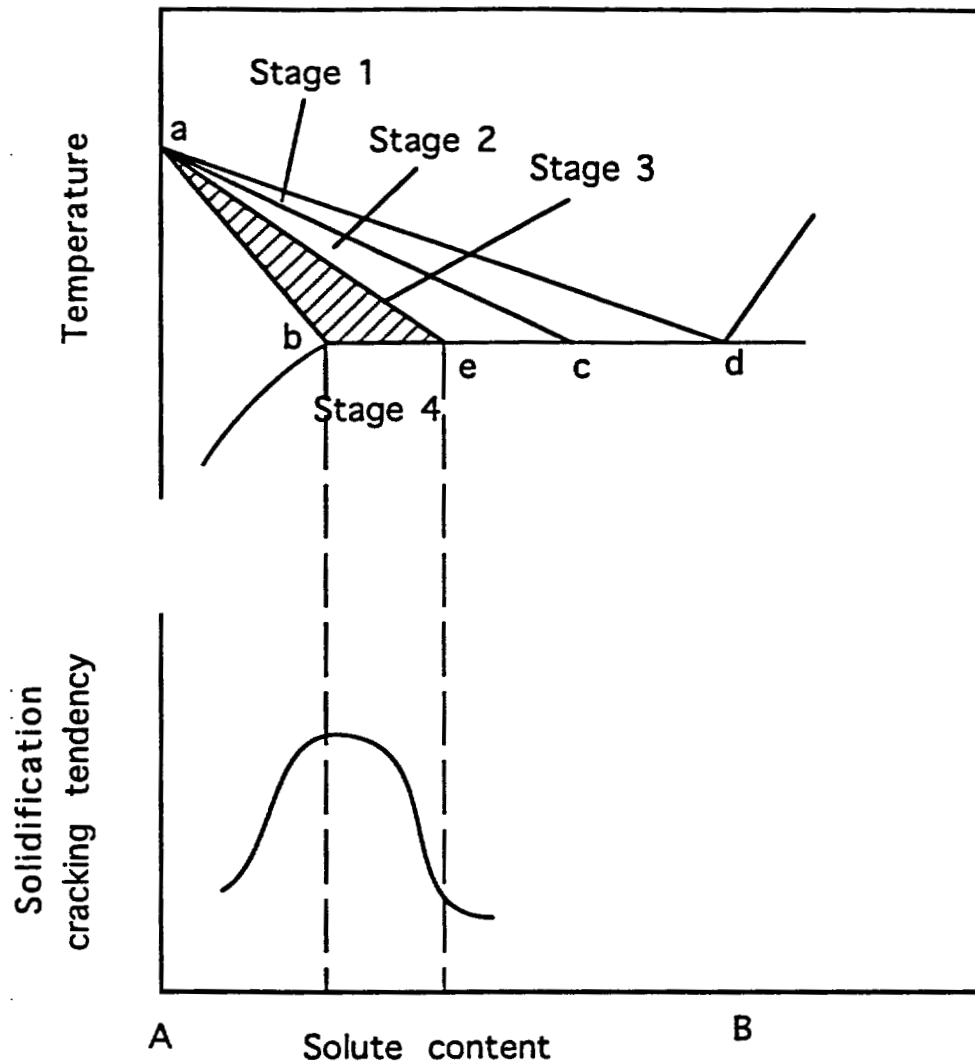
Figure 5. Four stages of hot cracking susceptability. a-c, coherent temperature; a-e, critical temperature; a-c-b, brittleness temperature range; Stage 1, dendrites freely dispersed in liquid, no cracking; Stage 2, solid-solid bonding, "liquid healing" possible if cracks forms; Stage 3, critical solidification range, no "healing" of cracks possible if fracture strain exceeded;Stage 4, solidification, no cracks.

present. Chubb and Billingham[59] investigated the ductility of cupronickel alloy at elevated temperature and indicated that for nickel contents of 18% and higher, the ductility fell sharply to a minimum at about 1000K. Above and below the ductility trough, fracture was by microvoid coalescence; in the trough itself the fractures were intergranular. They proposed that this intergranular failure was attributed to segregation of impurity atoms to the grain boundary. In their studies, the segregating element was suggested to be nickel itself.

CHAPTER 3
EXPERIMENTAL PROCEDURE

3.1 MATERIALS:

This study was based on a comparison of weldability between two 70/30 cupronickel claddings which were deposited by the same ESS process, but with different fluxes. All materials used for the two sets of welds were the same except for the fluxes. In order to simplify the following discussion, the cladding which was deposited with flux 1 was named cladding 1, similarly, the other was cladding 2 (Table 1). The details of materials are given in the following text.

Table 1. Classification of cupronickel claddings deposited on MIL-S-23284, Class 1 steel plate with 70Ni-30Cu buttering layer

	Flux	Crack
Cladding 1	1	yes
Cladding 2	2	No

Strip Electrodes

Two strips, 70 Cu-30Ni and 30Cu-70Ni, were used as the electrode materials in this study. The nominal compositions of these two materials are listed in Table 2. Both strips were the same size, 30mm wide by 0.5mm thick. The 70/30 cupronickel alloy was used to be a main welding material, while 70/30 nickelcopper alloy was used to be a buttering material to prevent the diffusion of iron atoms from base layer steel into the cupronickel weld metal.[17,52]

21

Table 2. Chemical compositions of 70Cu-30Ni strip, 30Cu-70Ni strip,
and the base metal steel (MIL-S-23284, Class 1)

Elements, wt%	70Cu-30Ni Strip	30Cu-70Ni Strip	Class 1 Steel
C	0.02	0.02	0.25
Fe	0.55	0.52	bal
Ni	31.25	65.10	3.252
Cr	-	-	0.427
Mo	-	-	0.442
Nb	-	-	0.003
Mn	0.73	3.54	0.335
Si	0.04	0.17	0.221
Cu	66.99	28.64	0.093
Ti	0.42	1.98	0.001
Al	<0.01	0.03	0.005
S	0.001	0.001	0.02
P	0.001	0.001	<0.001
Co	0.01	-	0.009
V	-	-	0.059
W	-	-	0.018
Mg	<0.01	-	-

Fluxes

For comparison purposes, two nearly similar commercial fluxes were used during the ESS process. The major chemical ingredients of the fluxes are shown in Table 3. Comparing the two fluxes, flux 1 did not contain the rare earth-containing material CeF_3 and the potassium-containing material K_2ZrF_6 and K_2SiO_3. The latter two materials were usually added to the flux for effective slag removal. The specific effect of the element Ce on the weldability of cupronickel alloy will be discussed in detail later.

Table 3. Major chemical ingredients of the fluxes

Ingredient	Flux 1 (wt%)	Flux 2 (wt%)
Al2O3	8	10
CaF2	80	70
SiO2	5	0.5
CeF3	-	10
K2ZrF6	-	3
MgO	-	3
Mn	-	2
K2SiO3	-	1.5
BaF2	6	-
K2O+Na2O	1	-

Substrate

The base plates onto which the two sets of claddings were deposited are the same material, a hardenable alloy steel (MIL-S-23284, Class 1). The nominal composition of this base plate is also listed in Table 2. The thickness of the plate was about 25mm.

3.2 ELECTROSLAG SURFACING (ESS) PROCESS:

Two sets of four layer weldments were deposited by ESS (Fig. 6) onto steel. The first layer 70Ni-30Cu alloy for both claddings were deposited by ESS onto the steel to "butter" the iron-base alloy. They were performed under the same working parameters as 700 amps, 30 volts, 7 in/min (17.8 cm/min) travel speed, 3.5 mm tie-in overlap and 30-35mm tip-to-work distance (Table 4). Four passes were deposited in this layer. Subsequent to the 70Ni-30Cu alloy, three layers of 70Cu-30Ni main welding material were deposited onto the buttering nickel base alloy. Two fluxes with their own optimum welding parameters (Table 4) were used for these two claddings. In the first two cupronickel layers, three passes were deposited. The last layer contained two passes as shown in Figure 6. 3.5mm tie-in overlap was applied to join two adjacent passes.

Table 4. Electroslag Surfacing Parameters

	Buttering Layer	Cupronickel Layer	Cupronickel Layer
	Flux 1	Flux 1	Flux 2
Voltage (Vots)	30	26.5	25
Current (Amps)	700	625	900
Travel Speed(Ipm)	7	7	9.5
Heat Input(kJ/in)	180	142	142
Crack	No	Yes	No

70Cu-30Ni

30Cu-70Ni

Steel Base Plate
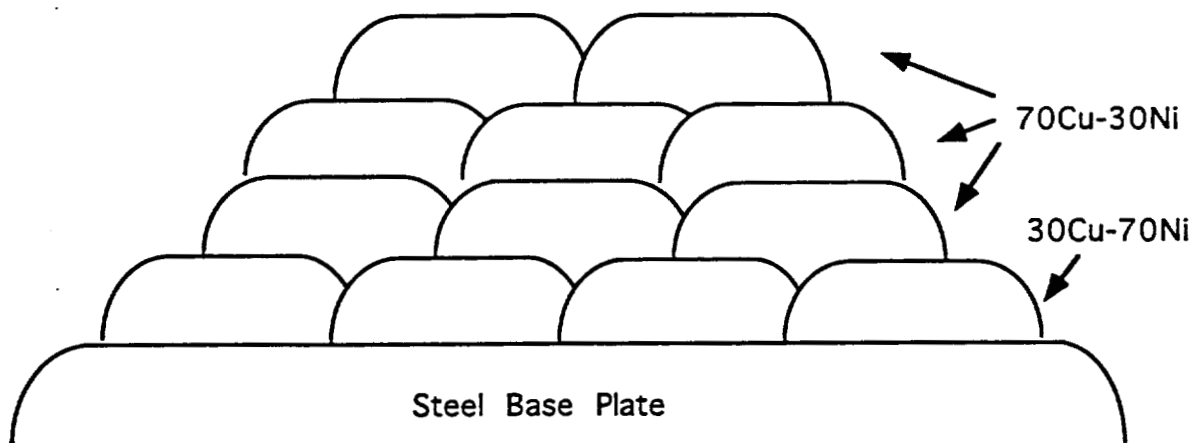
Figure 6. Schematic of the cross section of the multi-layer cupronickel
cladding using a buttering layer of 70Ni-30Cu deposited on
MIL-S-23284, Class 1 steel

3.3 METALLOGRAPHY OF CLADDING:

Optical Microscopy

Two sections of weldment were cut from both claddings. The welds were then briefly polished to reveal microcracks if any. The distribution and morphology of microcracks were observed and photographed with a Nikon SMZ-U optical microscope. The welds were then sectioned in two directions: (1) perpendicular to the top surface and parallel to the welding direction, and (2) parallel to the top surface. These specimens were then prepared for metallographic analysis by mounting them in epoxy and polishing through 0.05 μm alumina. An acidic $FeCl_3$ was used to reveal the solidification substructure and grain boundaries. Image analysis was performed with Nikon Epiphot microscope and LECO2001 Image Analysis System.

Scanning Electron Microscopy (SEM)

After the initial optical observation, the specimens were examined in a scanning electron microscope (SEM). The line scans across dendrites and grain boundaries were obtained with a Zeiss DSM 960 Digital Scanning Electron Microscope (SEM) which was equipped with an energy dispersive X-ray spectroscope (EDS) and a Link eXLII Analytical System. The compositions of inclusions and slags were obtained with the same equipment and calculated using Semiquantitative Analysis (SSQ) program. The SEM operating voltage for all the experiments was 20 kv.

Transmission Electron Microscopy (TEM)

In order to compare the precipitates from different claddings, an extraction replica technique was used. To prepare the samples, the polished optical specimens were electroetched in 10% oxalic acid to reveal the microstructure, and then carbon coated in an evaporator, followed by another electroetching in 10% HCl/methanol acid to relieve the coating film with the precipitates embedded inside. The carbon films were then supported on the 3mm diameter gold mesh grids.

The prepared TEM specimens were examined in the Hitachi H-800 Electron Microscope at 200 kV which was equipped with a low-take-off angle X-ray detector and a Tracor Northern TN2000 multichannel analyzer. Energy-dispersive spectroscopy (EDS) data were obtained in the STEM mode. Semi-quantitative compositions were obtained from EDS data via the standardless-ratio technique with a data reduction routine. Since the thin-foil conditions always applied, an absorption correction was not necessary.

3.4 FRACTOGRAPHY OF CLADDING:

Specimens from both claddings were tensile fractured in a room temperature in order to expose the crack surface. The crack surfaces were then observed with a scanning electron microscope (SEM) and elements on the crack surface were analyzed with an energy dispersive spectroscope (EDS) attached to the SEM. To obtain the profile of elemental distribution on the fracture surface, the average X-ray counts were detected every other 100 μm. Each average X-ray count was calculated based on three surface areas, each dimension of which was 20 $\times$ 20 μm^2 .

3.5 MECHANICAL TESTING:

Tensile test samples for both as-welded and as-stress relieved were cut from the cupronickel cladding layers of cladding 2. The gage length and the diameter of the tensile specimens were 50mm (2") and 12.7mm (0.5"), respectively. Tensile tests were performed at room temperature. The ultimate tensile strength (UTS), yield strength (YS), elongation and reduction of area were measured.

The Rockwell Standard microhardness was measured using a microhardness tester, with a 150kg load and a 1/16 in. ball. The specimens were polished using the metallographic specimen preparation procedures. Each specimen was tested ten times randomly at different layers of cupronickel cladding and the average data of the hardness was calculated.

CHAPTER 4

RESULTS

4.1 METALLOGRAPHIC EXAMINATION:

Microstructural Analysis

The optical micrographs of transverse cross-sections of both cladding 1 and cladding 2 are shown in Figure 7. A number of microcracks were observed in cladding 1 (Fig. 7a). These cracks occurred only in the 70/30 cupronickel weld metal and stopped right at the interface between cupronickel layer and nickel-copper layer. Most of the cracks were between two layers and had an orientation perpendicular to the welding direction and the top surface. This was associated with the grain growth direction and the direction of the contraction stresses. The degree of cracking decreased from 1st layer 70/30 cupronickel (most) to the 3rd layer (least). This was because the 1st layer cupronickel had more impurities diluted from the base metal and buttering layer, and more complicated conditions due to reheating by succeeding passes. Conversely, cladding 2 (Fig. 7b) had a perfect welding structure and was found free from cracking. This confirmed that the weldability of 70/30 cupronickel alloy could be improved by using different fluxes.

The microstructures of both cladding 1 and cladding 2 are shown in Figure 8. Basically, the solidification structure developed in cupronickel welds was a single phase dendritic structure (Fig. 8a, b). Compared with Fig 8c and d, the dendritic structure of both claddings was about the same. However, the grain boundaries in cladding 1 (Fig. 8c) were etched darker than cladding 2 (Fig.8d). This was related to impurities segregation. Furthermore, "chinese script" grain boundaries were observed in cladding 1 (Fig. 9a, b) which may be associated with the existence of $Cu-Cu_2O$ eutectics.

28
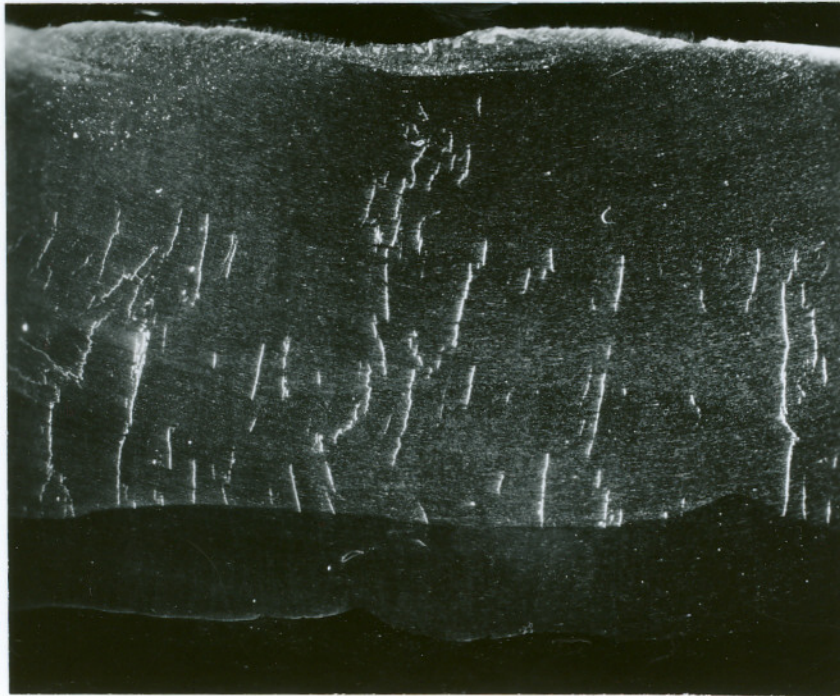
(a)
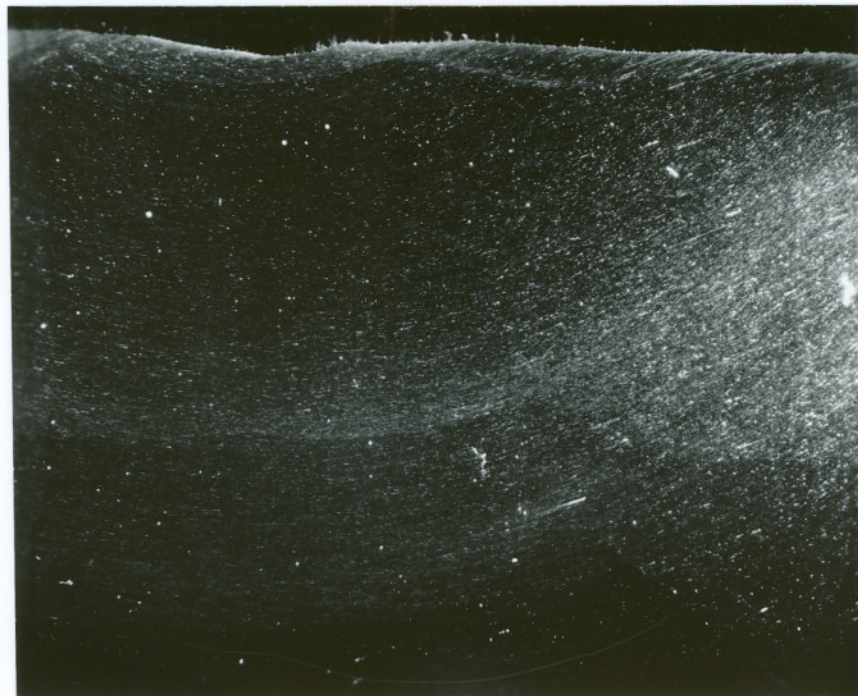
(b)

Figure 7. Cross-sections of weldments, 4x (a). cracking in cladding 1
(b). Sound deposit in cladding 2

(a)

(b)

(c)

(d)
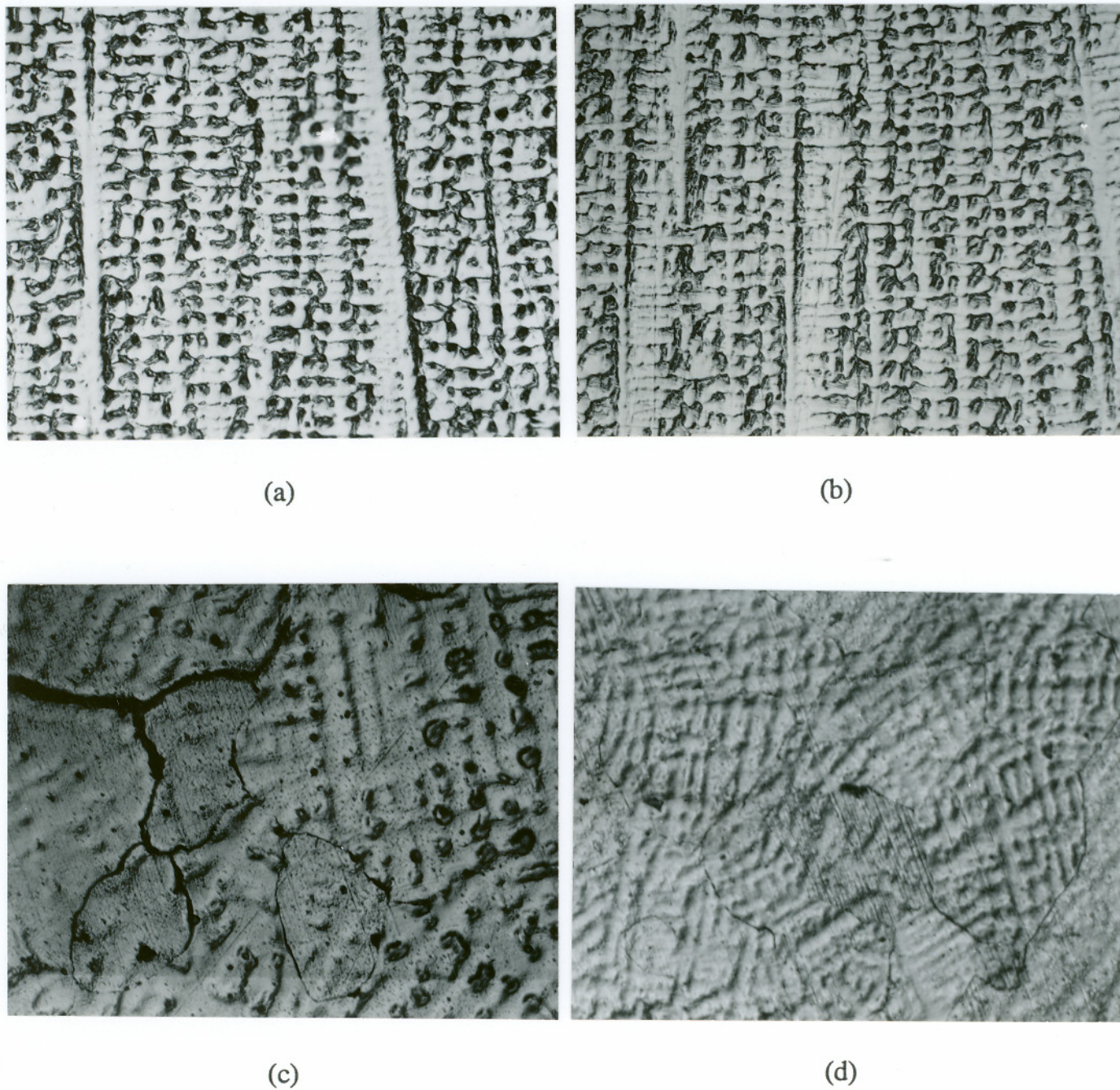
Figure 8. Dendritic structures of cupronickel claddings
      (a). General dendritic structure in cladding 1, 200x
      (b). General dendritic structure in cladding 2, 200x
      (c). The darker grain boundaries in cladding 1, 400x
      (d). The lighter grain boundaries in cladding 2, 400x
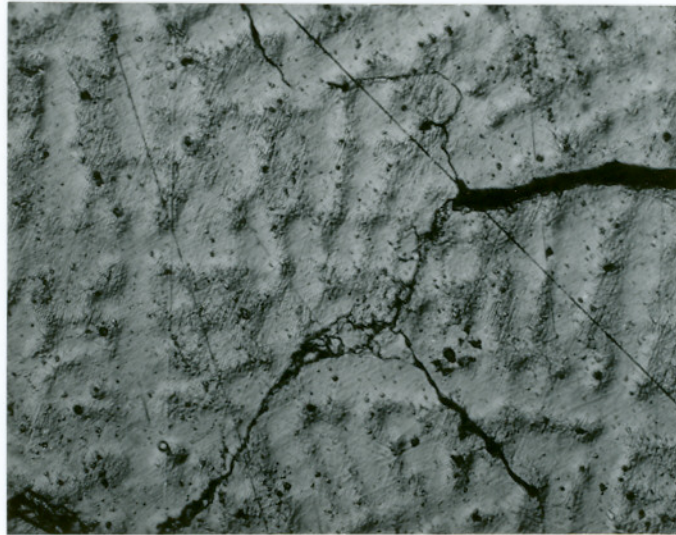
(a)
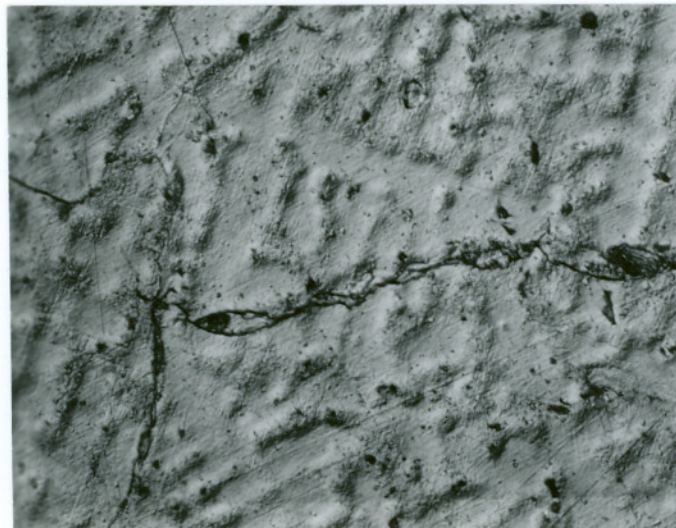
(b)

Figure 9. "Chinese Script" grain boundaries in cladding 1
showing the segregation of Cu-Cu$_2$O eutectic to the
grain boundaries, 400x

Comparing cladding 1 and 2, the major difference observed was cracking. As mentioned above, heavy cracking was observed in cladding 1 while cladding 2 was crack-free. Two features of hot cracking were found in cladding 1, that is, solidification cracking and ductility-dip cracking. As shown in Figure 10a, the cracking was along grain boundaries and separated grains which were in different orientations. Such crack was a direct result of the solidification process and known as solidification crack. As indicated later in fractographic examination, this cracking surface was decorated by liquid films which resulted from microsegregation. As shown in Figure 10b, the crack cut across the solidification structure but did follow grain boundaries which had migrated across the solidification structure. The crack of migrated grain boundaries was free from films. Such crack was a result of ductility-dip and known as ductility-dip cracking. The migrated grain boundary is shown in detail in Figure 11.

Image Analysis

The metallographic specimens taken from both cladding 1 and 2 in the middle of the 1st layer cupronickel were examined with an image analysis system. The area fraction and the average size of the precipitates shown in Figure 12 were measured. For cladding 1, the precipitate area fraction was about 0.4%, while the precipitate area fraction in cladding 2 was about 0.6% which was 1.5 times as much as those in cladding 1. The average precipitate size in cladding 1 was about 3.0 μm^2, and the average size in cladding 2 was about 2.5 μm^2. The results indicated that precipitates in cladding 1 had less area fraction but had a bigger average size than those in cladding 2.

Extraction Technique

The extraction replica technique was used to determine the phase compositions in both cladding 1 and 2. Compared to the SEM/EDS technique, the extraction replica could provide more accurate chemical information from the precipitates by eliminating the influence from the surrounding matrix.
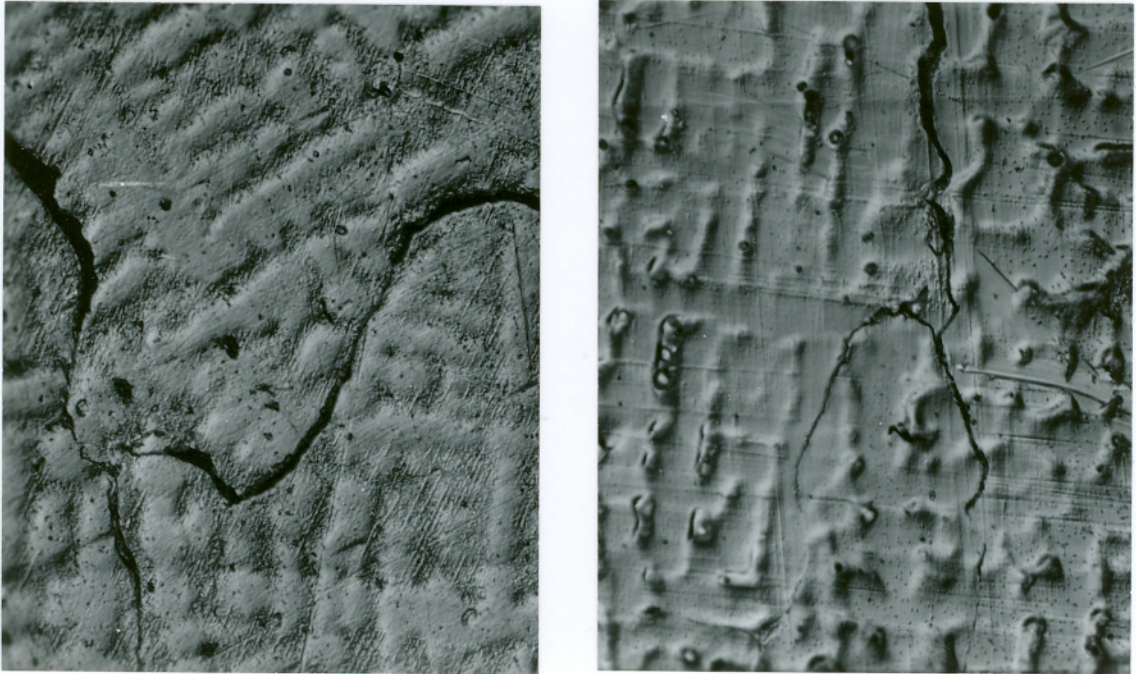
(a)
(b)

Figure 10. Hot cracking in cladding 1. 400x
(a). Solidification cracking
(b). Ductility-dip cracking
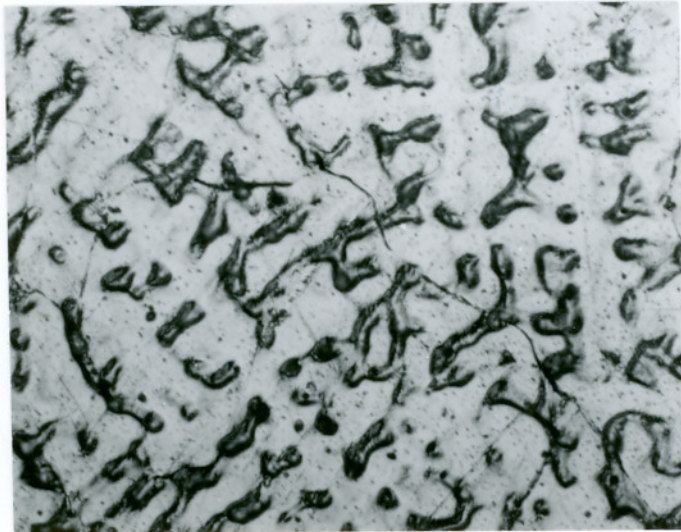
Figure 11. Migrated grain boundary in cladding 1. 400x

(a)

(b)

Figure 12. Backscatted electron images of precipitates in both
(a). cladding 1, and (b) cladding 2. 400x

Figure 13 shows TEM photos of extraction replicas obtained from cladding 1 surface. Two kinds of inclusions were observed in cladding 1. Those with a smooth round shape were (Al,Ti)-rich inclusions and those with an irregular shape were Si-rich inclusions. The energy dispersive X-ray spectra of (Al,Ti)-rich and Si-rich inclusions are shown in Figure 14a and b. The Au peaks were from the gold TEM grids, and can be ignored when analyzing chemical composition. For (Al,Ti)-rich inclusions, Ti had strong intensity peak besides the strongest Al peak. For the Si-rich inclusions, Si and Al were shown to be the two major elements. Due to the equipment limitation, the oxygen contents which were observed in the SEM results (Fig. 18) could not be determined in this method. Basically, the inclusions in cladding 1 were (M)O type oxides.

The inclusions in cladding 2 were similar to the oxides in cladding 1, but the compositions were slightly different. The TEM photograph of the extraction replica, Figure 15, obtained from cladding 2 shows the morphologies of precipitates. The appearance of inclusions looks similar to those in cladding 1, but the size in cladding 2 was smaller than those in cladding 1. According to the energy dispersive X-ray spectra (Fig. 16), the inclusions in cladding 2 were found in three forms. One is (Al,Ti)-rich oxide. Compared to those in cladding 1, this inclusion contained some sulphur which was not found in cladding 1 and more Ti and Mg content than those in cladding 1. The second type is the Si-rich inclusions. The last one is Ce-containing complex compound. Based on the X-ray spectra shown in Figure 16c, this compound was found to contain large amounts of Al, Ti, Ce, and trace amounts of Mg, Si, P, S and Ca.

Chemical Analysis

Elemental segregation was observed in the weld metal of cladding 1. Figure 17a shows a line scan profile obtained from the weld metal of cladding 1. According to the line scan profile, Cu, Ti, Al and Si concentrations were maximum in the interdendritic regions whereas Ni and Fe were at their minimum in these positions. This indicated that Cu, Ti, Al and Si tended to segregate to the interdendritic region. In addition to the continuous segregation pattern, the discontinuous elemental concentrations, namely
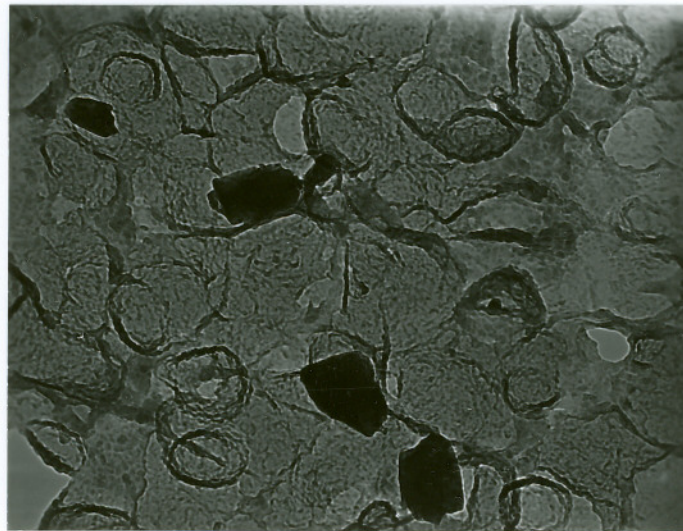
3μm

Figure 13. Extraction replica obtained from cladding 1 showing two kinds of inclusions. Those with a smooth round shape were (Al,Ti)-rich inclusions and those with an irregular shape were Si-rich inclusions.

(Al,Ti)-rich inclusion

(a)
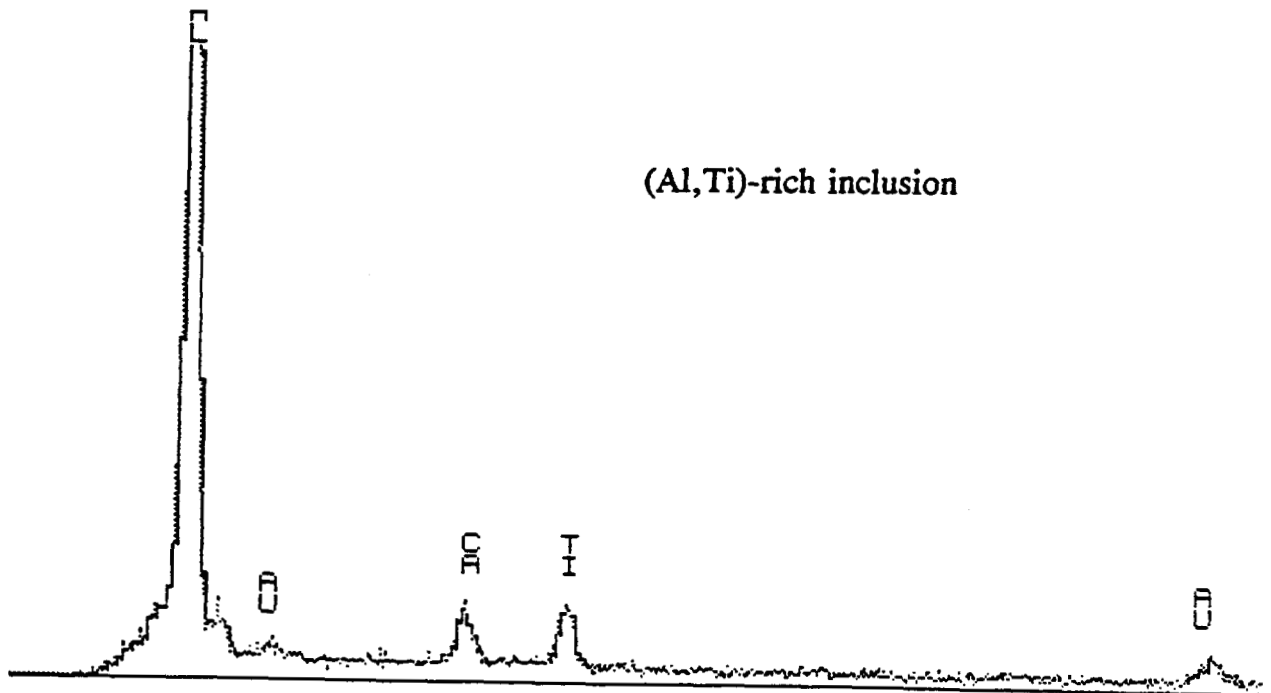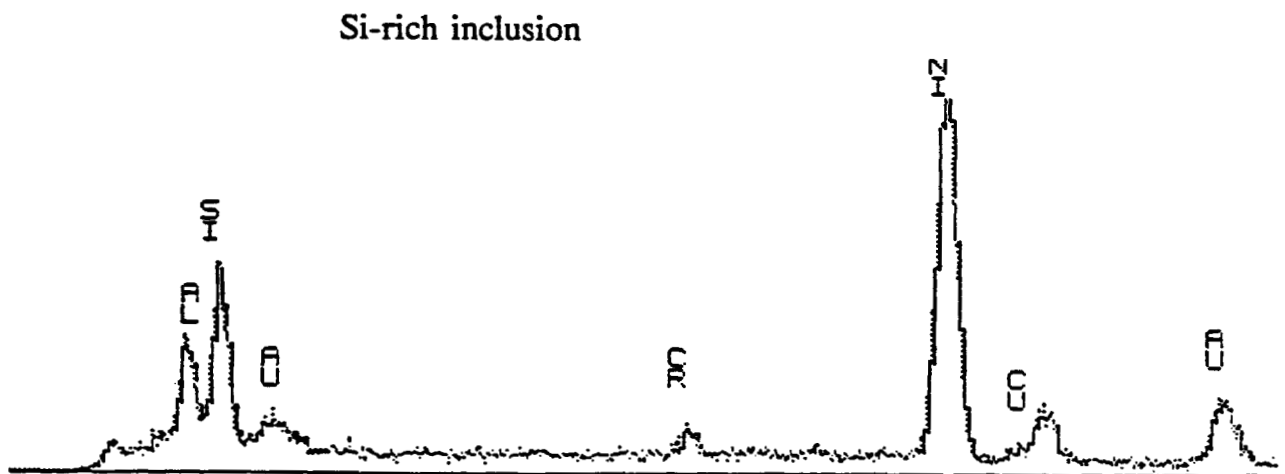
Si-rich inclusion

(b)

Figure 14. TEM/EDS spectra of inclusions in cladding 1.
(a). (Al,Ti)-rich inclusions
(b). Si-rich inclusions

3µm

Figure 15. Extraction replica obtained from cladding 2 showing
inclusions similar to Figure 13.

Figure 16. TEM/EDS spectra of inclusions in cladding 2
     (a). (Al,Ti)-rich inclusions
     (b). Si-rich inclusion
     (c). Ce containing complex compound

inclusions, were also observed. Figures 18a and b show representative X-ray spectra obtained from two typical inclusions. In Figure 18a, the inclusion was identified to be a (Al,Ti)-rich oxide, while that in Figure 19b was identified to be a Si-rich inclusion.

In contrast to cladding 1, the line scan profile (Fig. 17b) of cladding 2 shows a different segregation partitioning profile. In this case, trace elements Ti, Al and Si as well as Ni and Fe had minimum concentrations in interdendritic regions. This phenomena indicated that Ti, Al and Si have changed their partitioning distribution when clad with different fluxes. Detailed discussion about the reason will be presented in next section. In cladding 2, inclusions were observed distributing randomly within the cladding. With EDS, the inclusions were identified as (Al,Ti)-rich inclusions, Si-rich inclusions, and Ce-containing complex oxides. The representative X-ray spectra of these inclusions are shown in Figure 19.

4.2 FRACTOGRAPHIC EXAMINATION:

The tensile fracture surfaces of both cladding 1 and 2 were examined by SEM. Figure 20a showed the general appearance of hot cracking in cladding 1 where the intergranular fracture was elongated unidirectionally due to columnar grain growth. The solidification structure was not obvious to see due to the complicated conditions presented during multi-layer cladding. However, two types of hot cracking features were observed on the crack surfaces. Figure 20b shows a smooth fracture surface which was related to the existing of liquid film. This smooth free surface indicated that such cracking must occur above the solidus temperature and was related to solidification cracking. Figure 20c shows a fracture surface which was relatively rough compare to Figure 20b. No liquid films were observed in this region. The detailed observation revealed that thermal faceting existed (Fig 20d), which was a typical feature of ductility-dip cracking. All these observation indicated that a free surface existed at elevated temperature but after solidification.

Cladding 2 showed a totally different fracture mechanism. The fracture surface
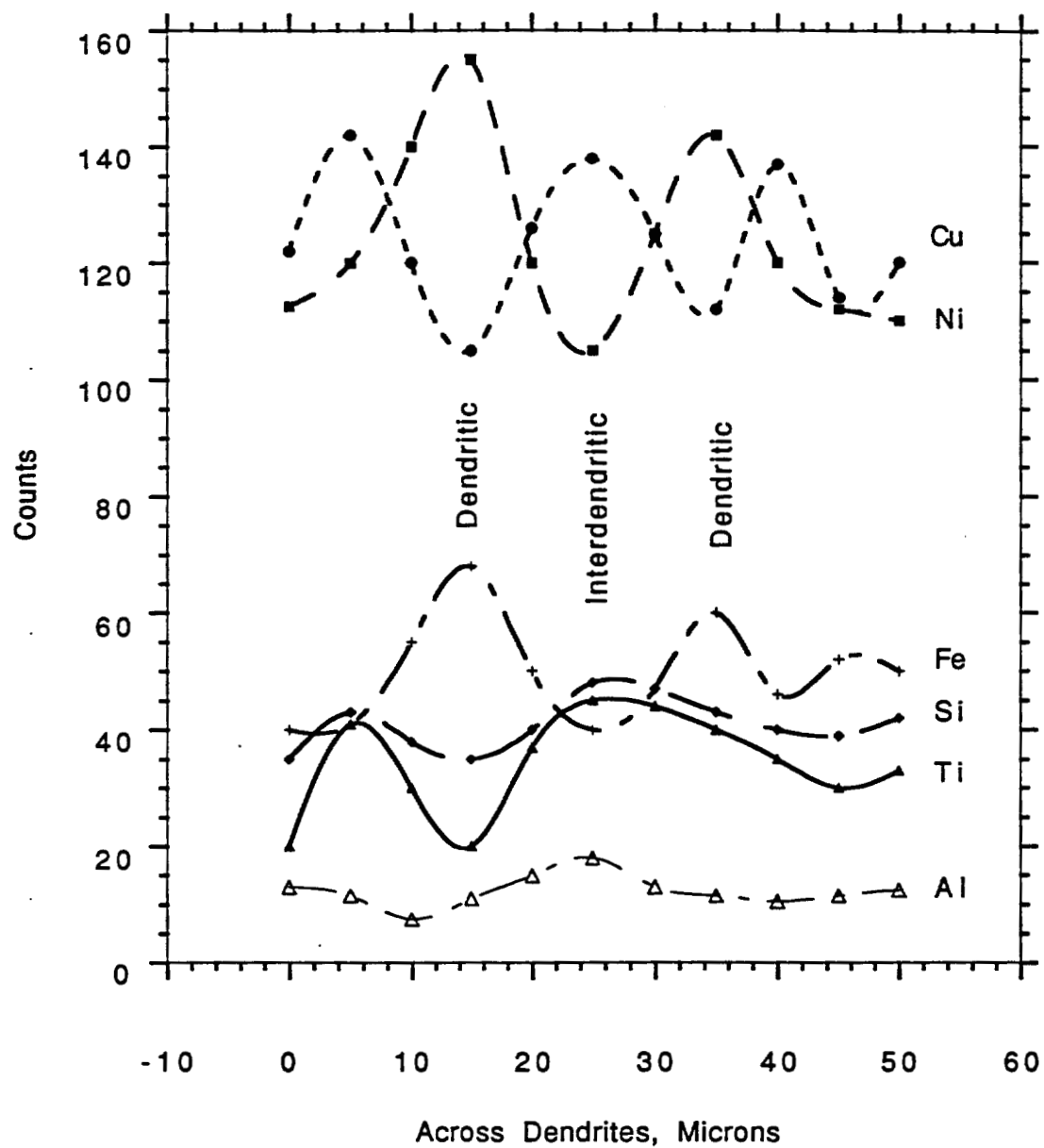
Figure 17 (a). Linescan profiles across dendrites in cladding 1
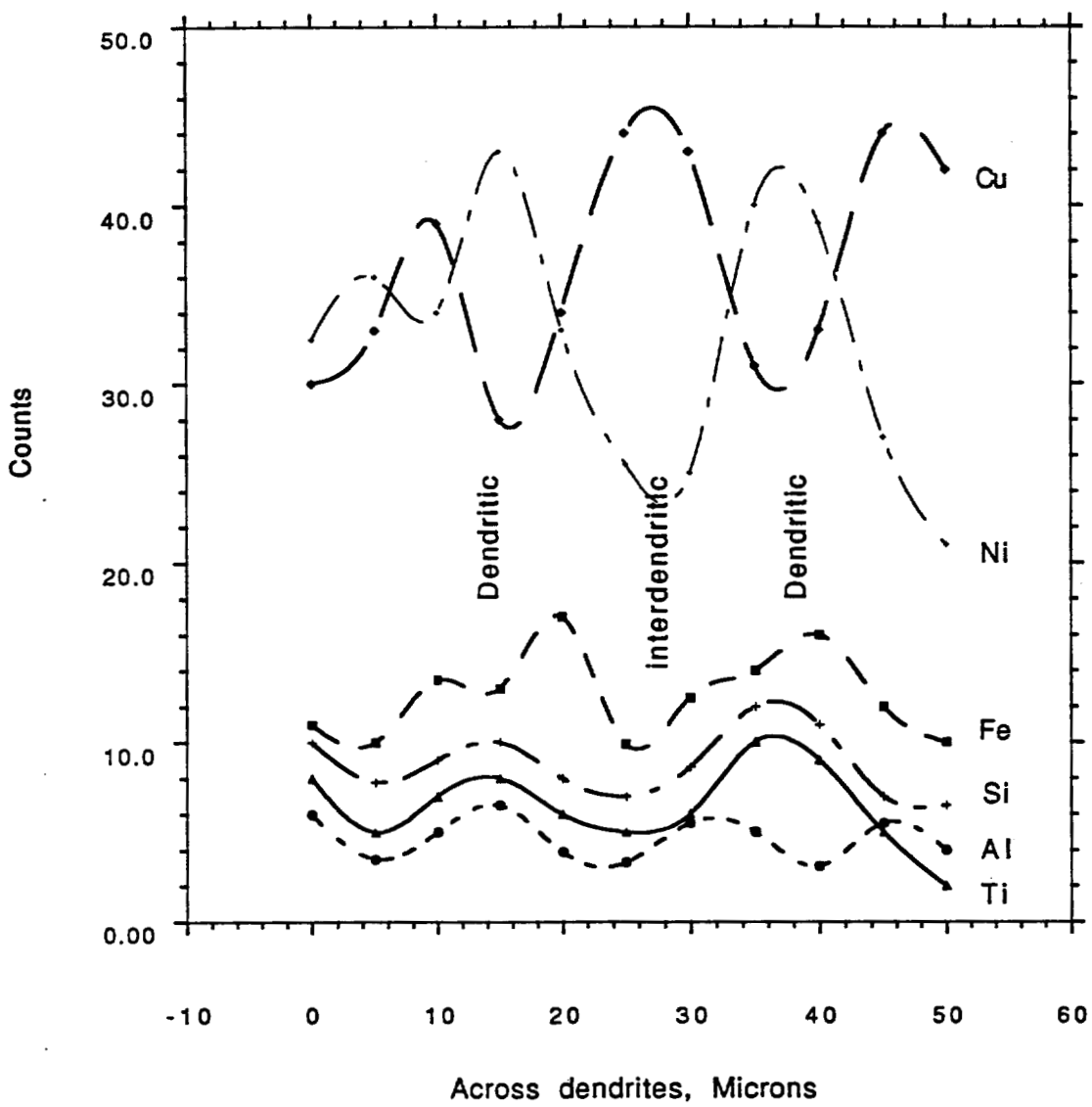
Figure 17(b). Linescan profiles across dendrites in cladding 2

(Al,Ti)-rich inclusion

(a)
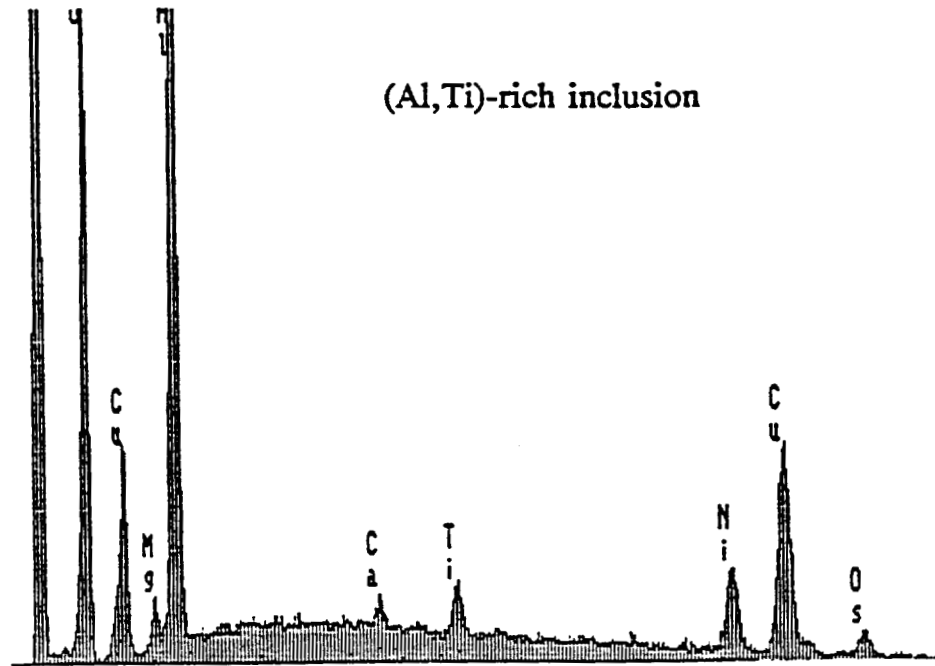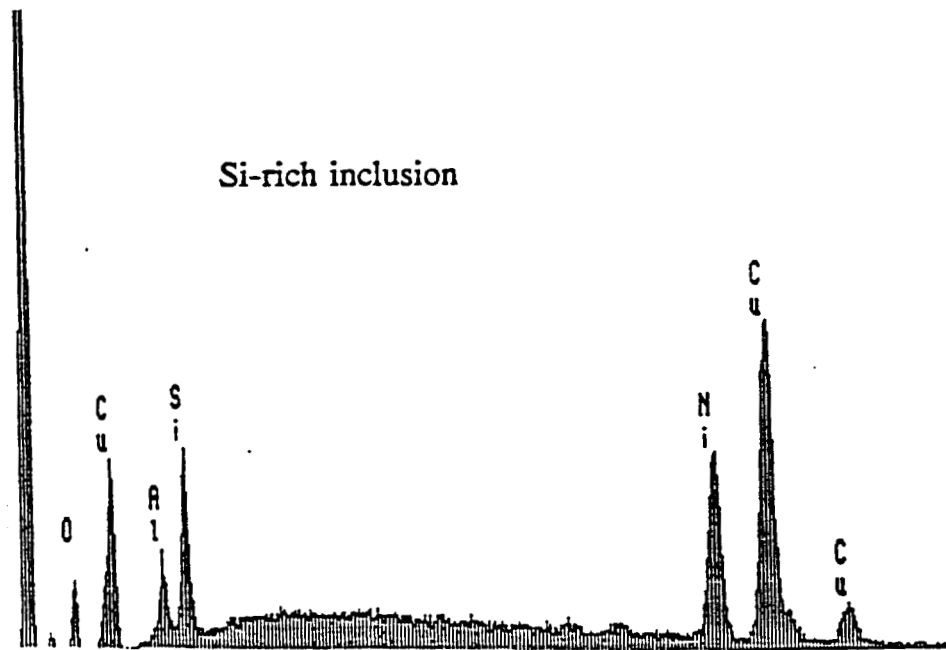
Si-rich inclusion
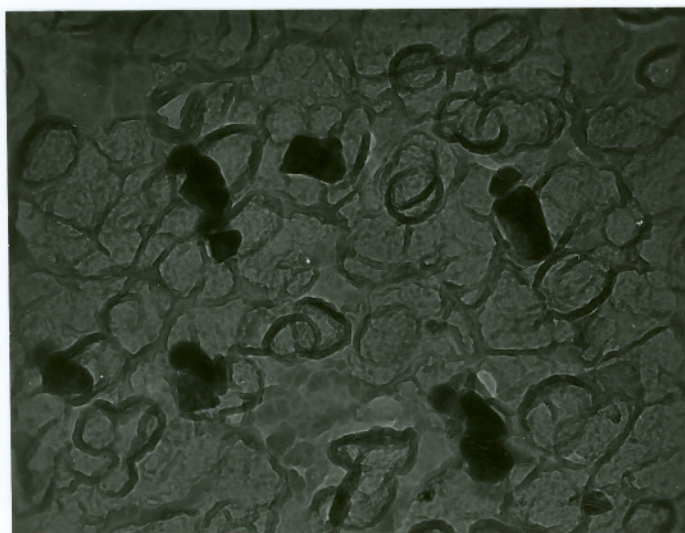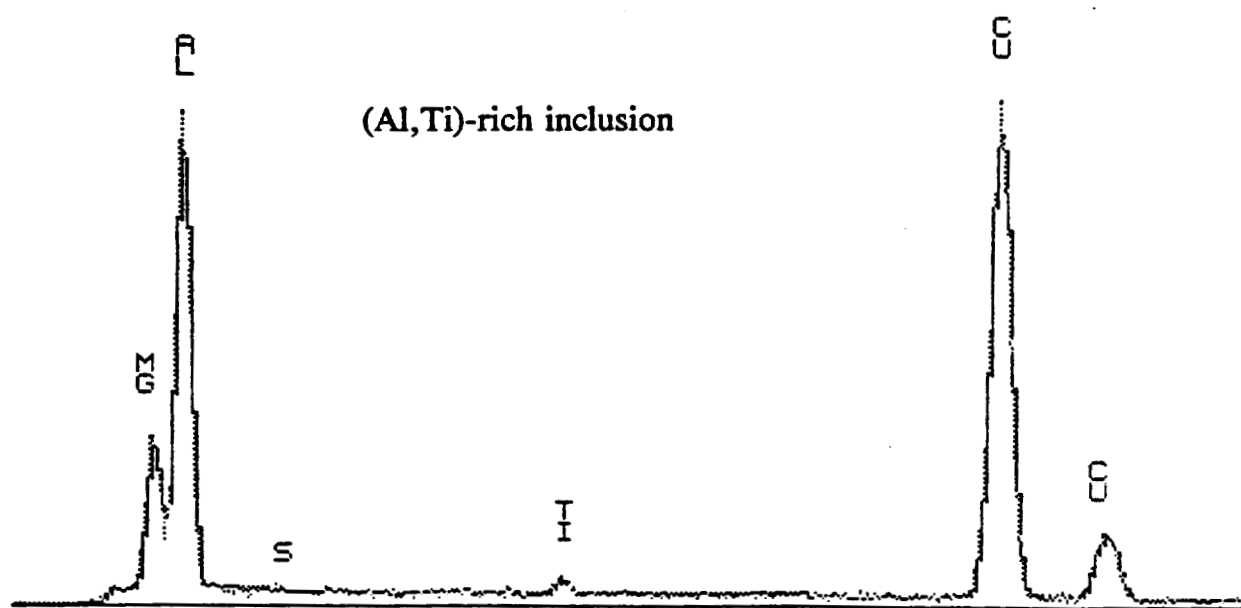
(b)

Figure 18. SEM/EDS spectra of inclusions in cladding 1
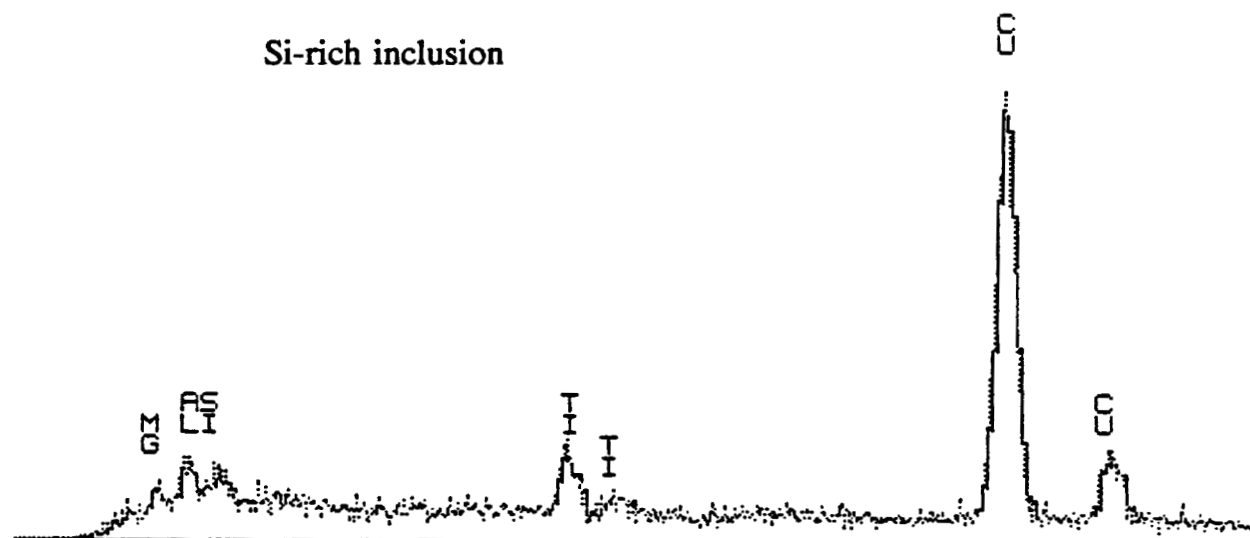(a). (Al,Ti)-rich inclusion
(b). Si-rich inclusion
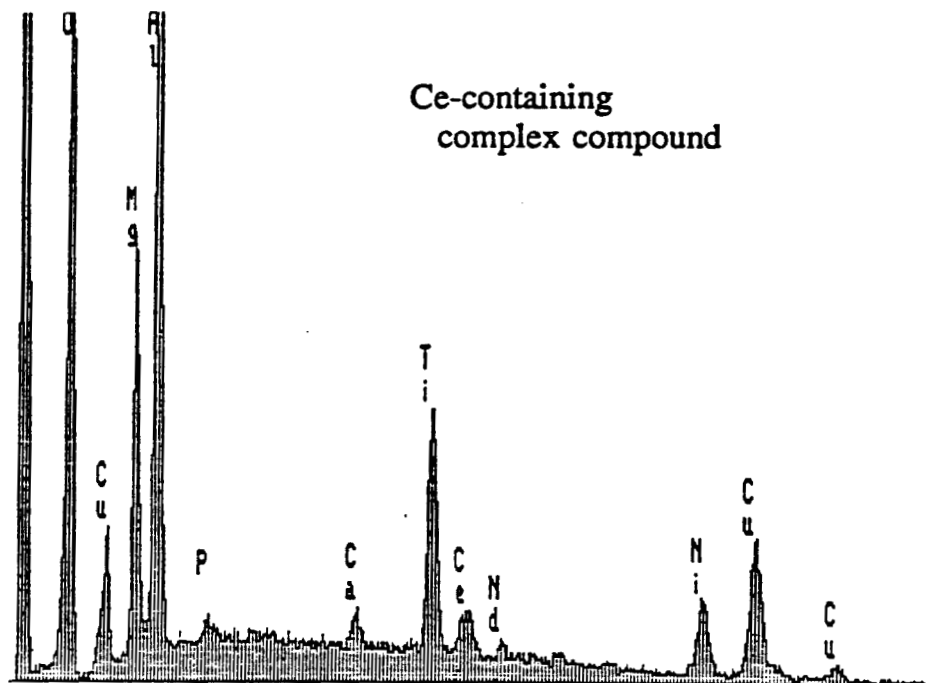
(a)
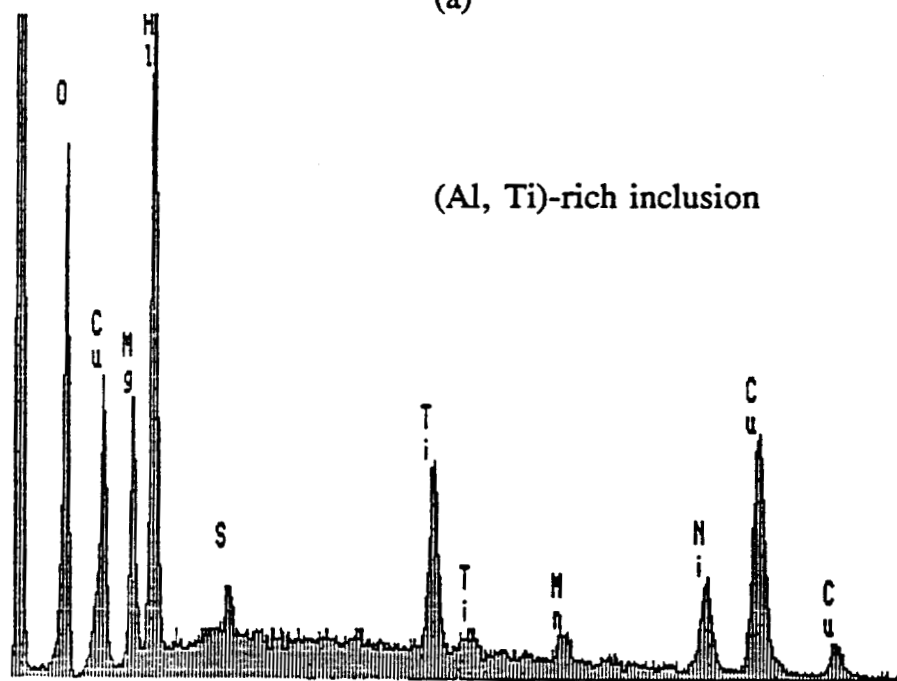
(b)

Figure 19. SEM/EDS spectra of inclusions in cladding 2
(a). Ce-containing complex compound
(b). (Al,Ti)-rich inclusion
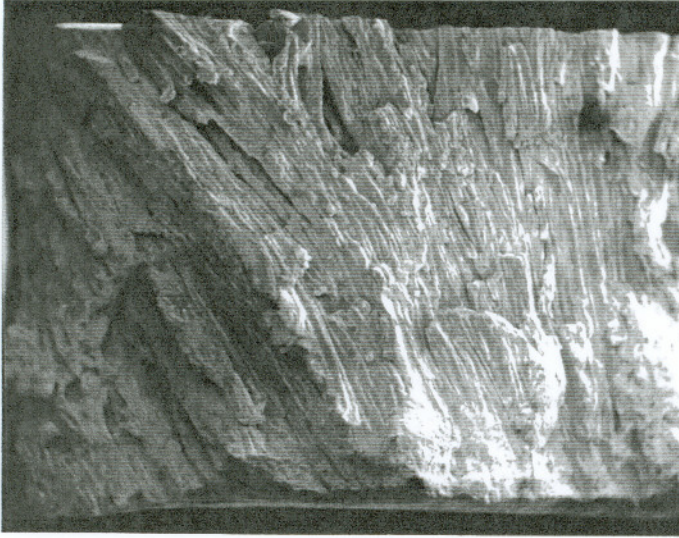
(a)
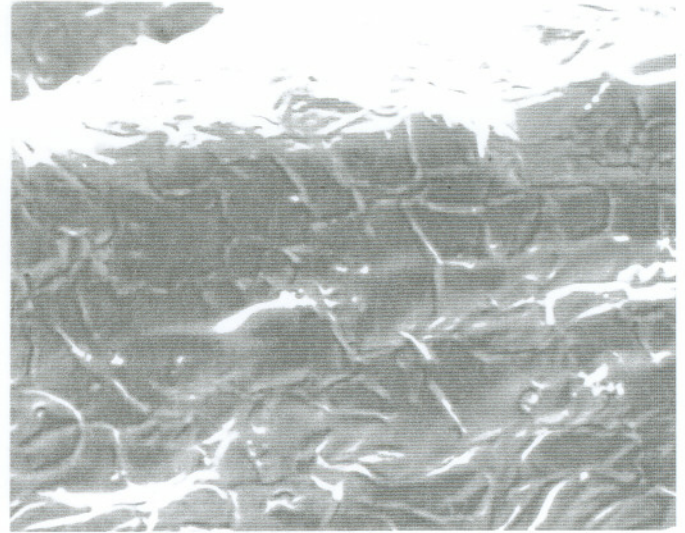
(b)
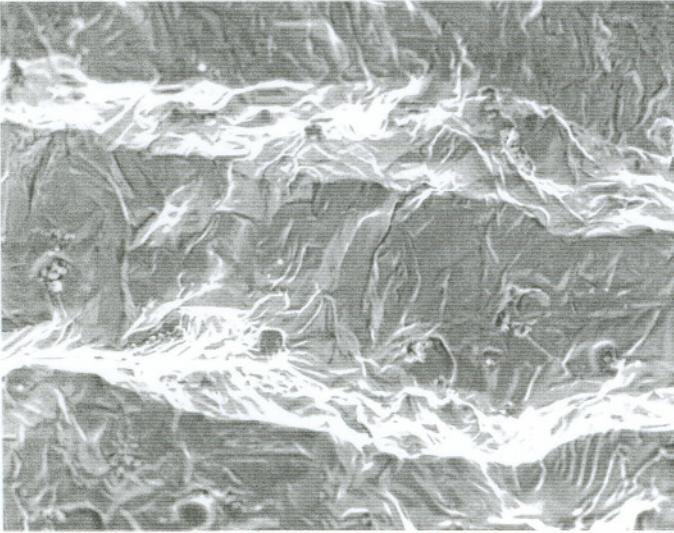
(c)
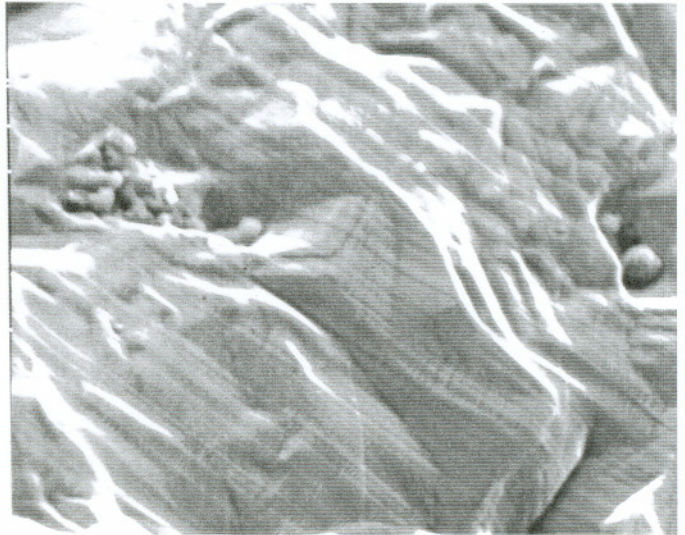
(d)

Figure 20. The appearance of hot cracking in cupronickel alloy
in cladding 1.
(a). General appearance of hot cracking, 10x
(b). Solidification cracking surface, 2000x
(c). Ductility-dip cracking surface, 1000x
(d). High magnification of ductility-dip cracking, 4500x
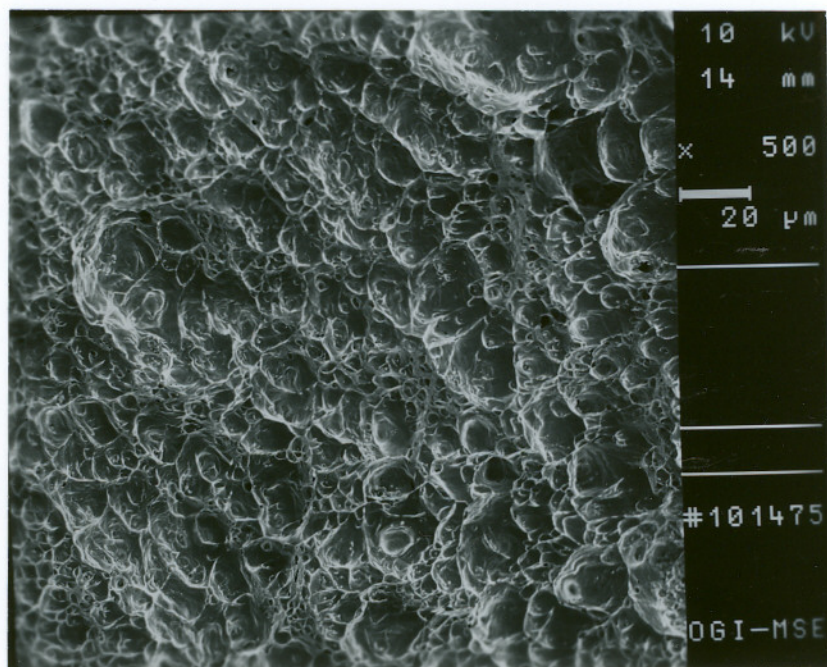
Figure 21. SEM fractograph, showing the ductile dimple
fracture surface of cladding 2

which exhibited a homogeneously distributed dimple structure (Fig. 21) indicated that no initial microcracking existed before the alloy being tensile fractured. In the other words, it confirmed that there was no hot cracking in cladding 2 prior to tensile testing. The ductile dimples were understood to be caused by inclusion nucleated voids.

On the cracked surface of cladding 1, two kinds of inclusions were observed. Sulphur-rich inclusions were found to be small in size with an irregular shape (Fig. 22a). Aluminum-rich inclusions were found to be round in shape, but in most cases, several inclusions were observed to be stuck together and giving the impression of a large size (Fig. 22b). The morphology of these two types of inclusions are shown in Figure 22a and b. The representative X-ray spectra of these two types of inclusions are shown in Figure 23. Sulphur-rich inclusions were shown to be high in S and Al content with a small amount of Fe, Mn, and Ti. Aluminum-rich inclusions were found containing high concentrations of Al, Ti, and a small amount of Mg, Ca, Fe, Mn.

Inclusions were also observed in the fracture dimples on the fracture surfaces of cladding 2 (Fig 24). With energy dispersive X-ray analysis, the inclusions were detected to be Ce-containing complex oxides and (Al,Ti)-rich oxides. These inclusions were the same types as those observed in metallographic specimens of cladding 2.

Elemental segregation was always considered relating to hot cracking. Therefore, the distribution of elements on the crack surface was investigated with EDS. For this purpose, the average X-ray counts were detected from three surface areas, each dimension of which was $20 \times 20 \ \mu m^2$ in area. In cladding 1, the distribution of elements were carried out across the cracking surface and tensile fractured area, as shown in Figure 25a. The results are shown in Figure 25b. The chemical compositions of elements changed from artificially fractured dimple area to crack area. The titanium content was increased from 0.4% wt in the dimpled area to about 0.15% wt in the cracked area, while Al and Si increased slightly. The elements with content less than 0.01% could not be detected. Therefore, the distribution of trace elements P, S, Mg etc. were not measured in this case. These chemical composition profiles indicated that titanium had a trend to segregate toward the interdendritic region and grain boundaries during weld solidification.
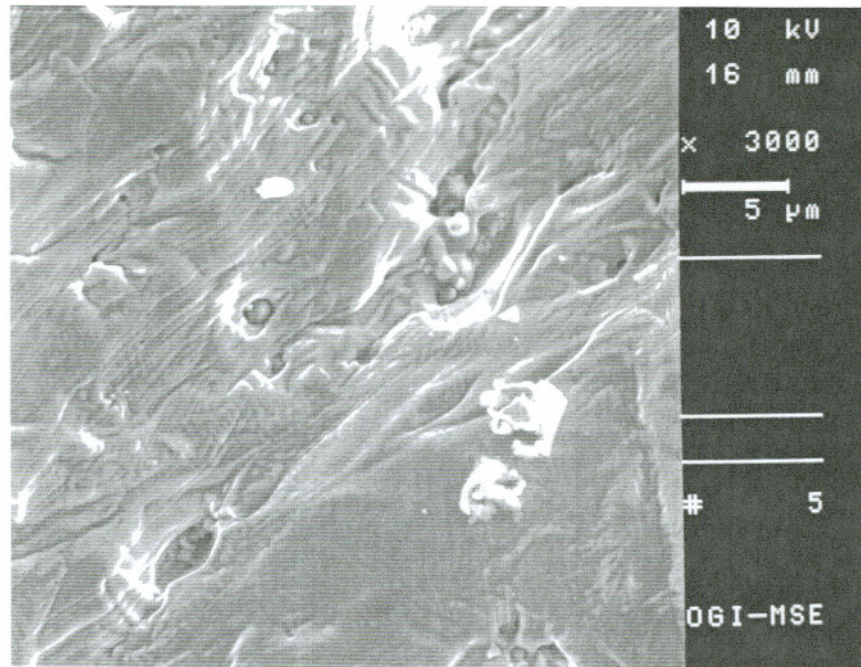
(a)
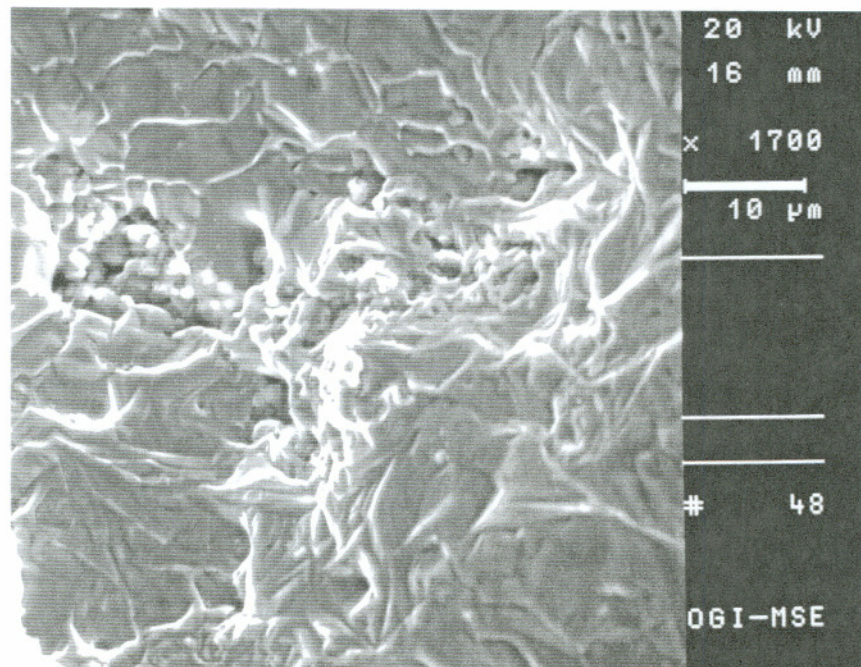
(b)

Figure 22. Inclusions at cracking surface of cladding 1
    (a). Round shape Al-rich inclusions and irregular
        shape S-rich incluaions
    (b). Bunch of Al-rich inclusions

S-rich inclusion

(a)
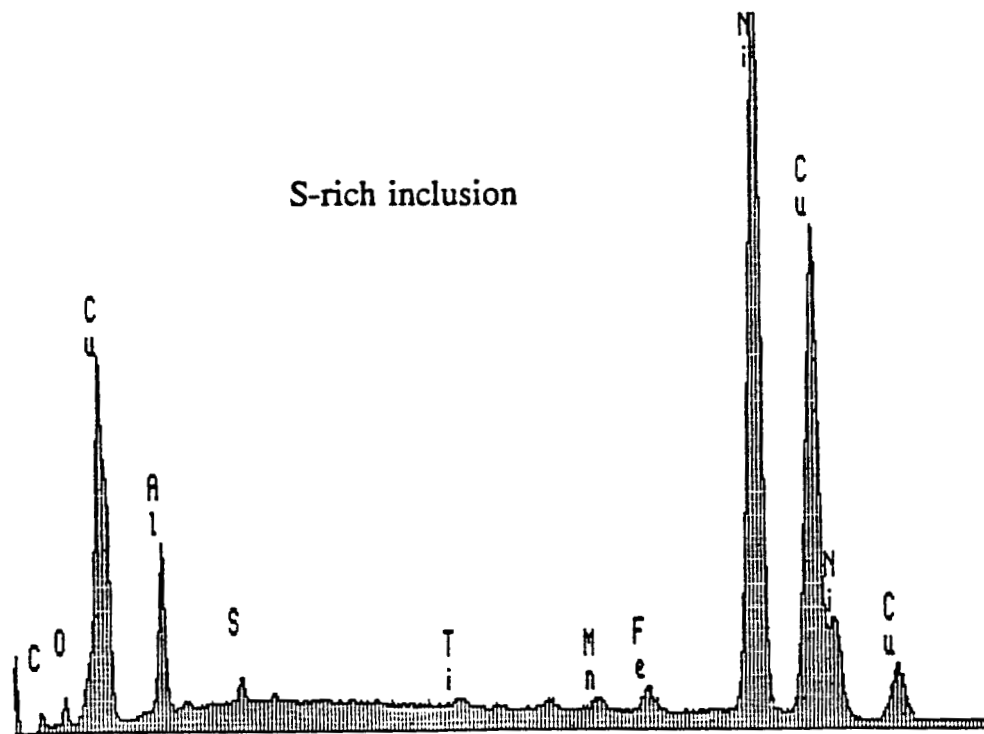
(Al, Ti)-rich inclusion
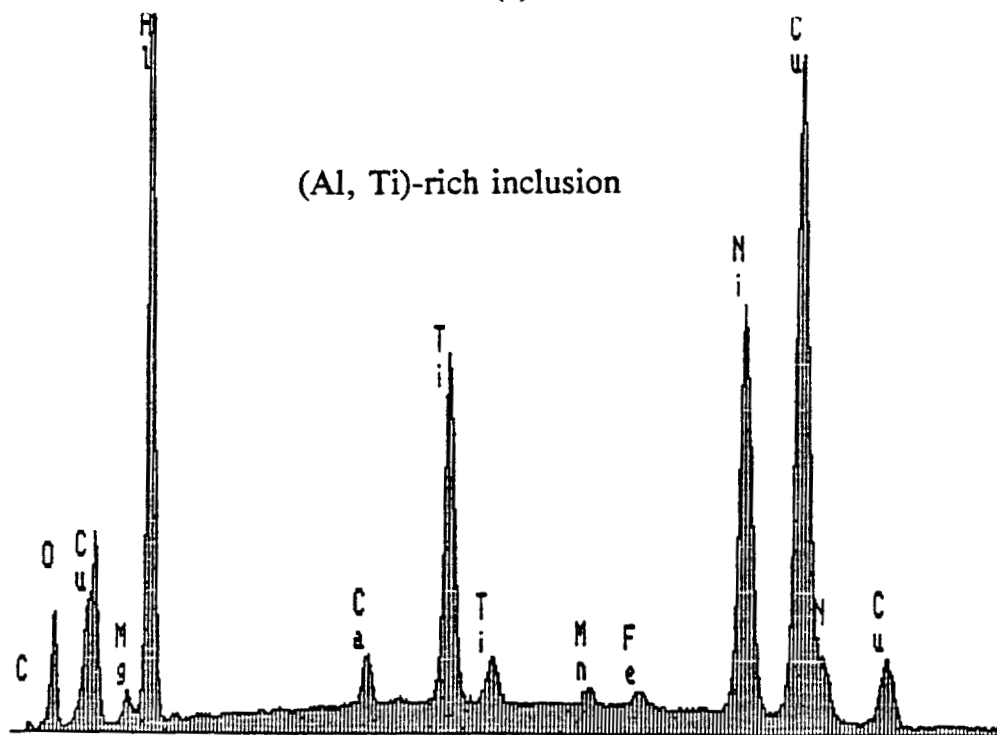
(b)

Figure 23. SEM/EDS spectra of inclusions at cracking
surface in cladding 1
(a). S-rich inclusion (b). (Al,Ti)-rich inclusion
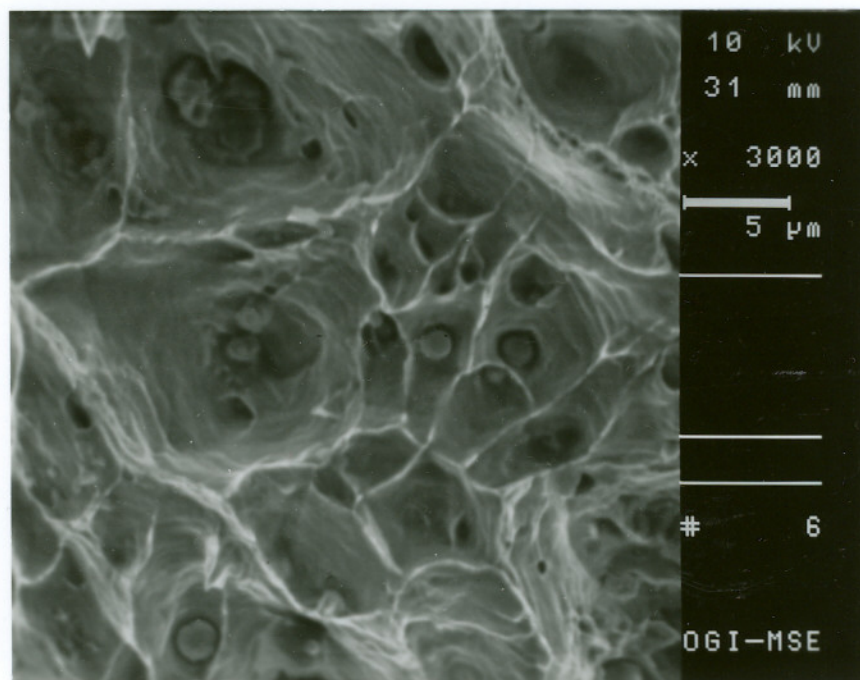
Figure 24. Inclusions at fracture dimples of cladding 2

Brittle fracture   Ductile fracture
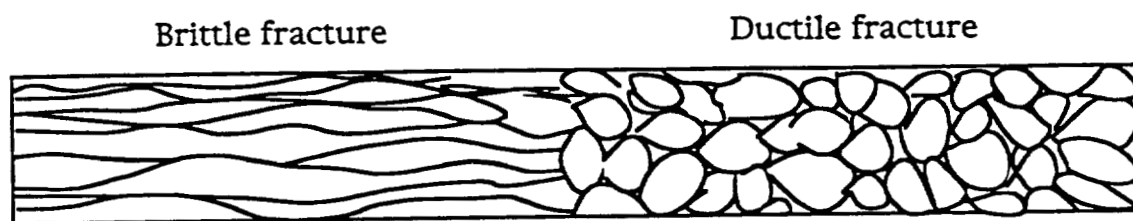
(a)
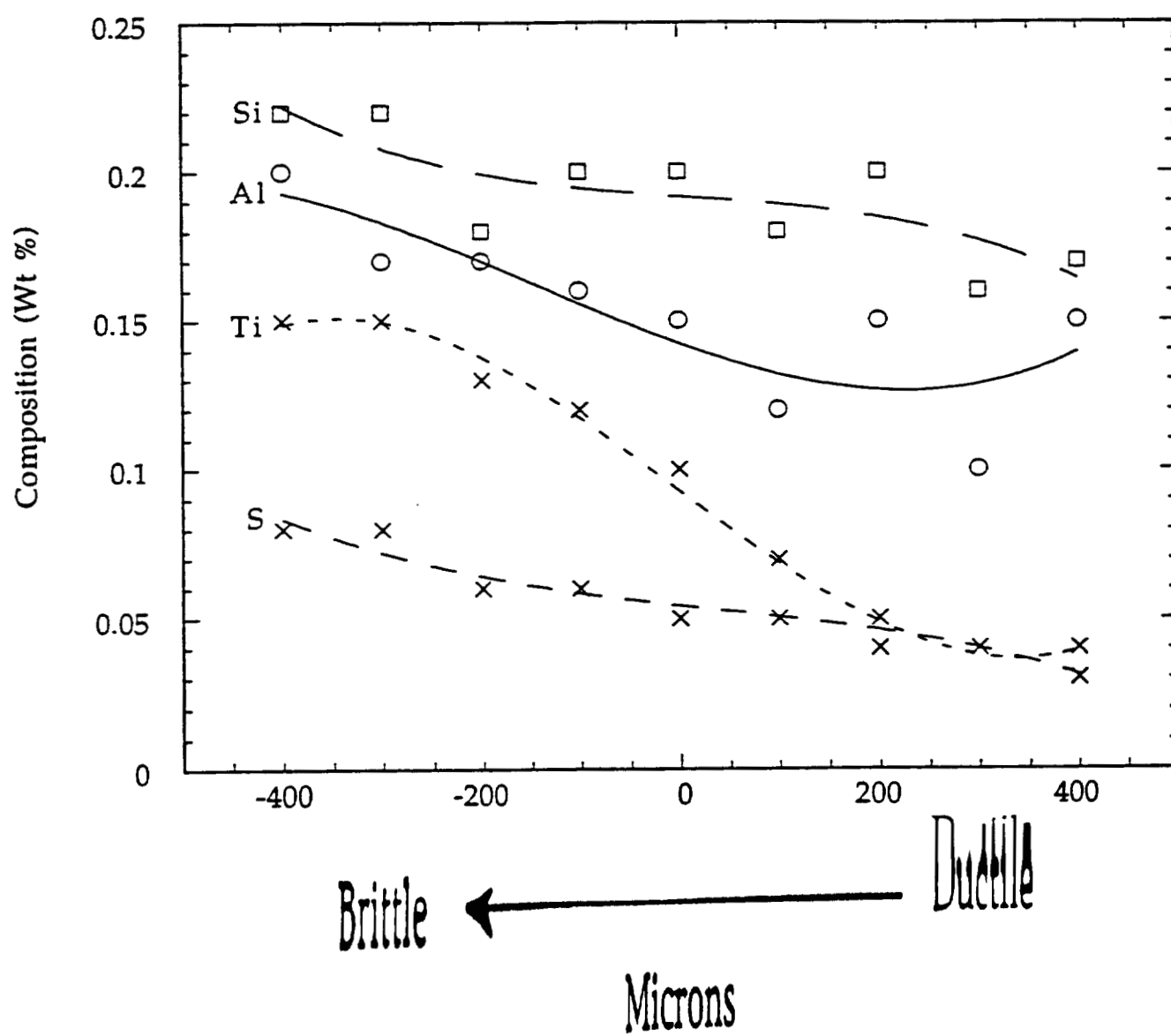
(b)

Figure 25. (a). Schematic of the fracture surface of cladding 1

The elemental distributions were also carried out in cladding 2. Since there were only artificially fractured dimple area, the average X-ray counts were detected in different locations. The results indicated that the contents of elements were nearly equal to the cladding composition.

4.3 MECHANICAL TESTING:

Tensile specimens were taken from cupronickel layers of cladding 1 and cladding 2 (as-welded and as-stress relieved) and were tested at room temperature. Essentially no tensile strength and no ductility was measured when testing cladding 1 due to the heavy cracking which existed prior to tensile tests. The results of tensile tests of cladding 2 in the as-welded and as-stress relieved conditions are shown in Table 5.

Table 5. The average mechanical properties and the associated standard deviation of cladding 2 at as-welded condition and as-stress relieved condition

	Condition	As-Welded		As-Stress Relieved	
		AVG	SD	AVG	SD
Tensile Properties	Yield Strength (ksi)	28.15	0.13	32.61	0.69
	Tensile Strength (ksi)	50.85	0.66	56.70	0.98
	% Elongation	30	1	27	3
	% Area Reduction	21.8	3.3	23	6
Rockwell Standard Microhardness (150kg, 1/16 inch ball)		29.6	1.1	33.6	0.9

Comparing the data shown in Table 5, the yield strength (YS) and the ultimate tensile strength (UTS) were slightly increased after the cladding being stress relieved.

The ductility decreased slightly from 30% elongation in the as-welded condition to 27% elongation in the as-stress relieved condition. Such phenomenon can be explained by Cu-O aging reaction. According to the chemical analysis, the oxygen content in cupronickel cladding was about 0.035% wt. A small amount of oxygen must dissolve in the cupronickel alloy. When heating this alloy to 650^{0}C for two hours, oxygen separated out from the matrix and formed Cu_2O (based on the Cu-O binary phase diagram)[57] with Cu. Once the second phase formed, it would block the movement of dislocations, therefore increased strength. However, the presence of Cu_2O would also brittle the grain boundaries and provide a weaker bond with the surrounding matrix, therefore reduced the material's capability of deforming plastically.

Further investigation in microhardness of cladding 2 in both as-welded and as-stress relieved conditions revealed the same results as tensile testing's, that is, the microhardness of cladding 2 at the as-stress relieved condition was higher than as-welded condition. The Rockwell Standard hardness of cladding 2 tested in a load of 150kg with a 1/16 inch ball at the as-welded condition was about 30 HB, while at the as-stress relieved condition was 33 HB (Table 5).

CHAPTER 5

DISCUSSION

5.1 MELTING CONSIDERATIONS:

When the cupronickel alloy melts during the ESS process, its chemical composition can be greatly influenced by the flux and base metal. Such compositional changes will greatly affect the structure and quality of the weldment. In the ESS process, the melting of filler and base metal is fulfilled by resistance heating of the slag pool. During the flux-shielded welding process, chemical reactions take place between the slag and the metal. This interaction will result in compositional changes in the resulting cladding.

According to previous researchers[32-39], the reaction between slag and metal is

$$xM + yO = (M_xO_y) \qquad\qquad 5.1$$
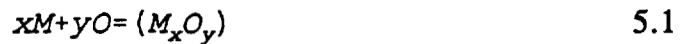
the equilibrium constant for the above reaction is

$$K_i = \frac{(a_{M_xO_y})}{[a_M]^x [a_O]^y} \qquad\qquad 5.2$$

The *reaction might either proceed forward* or backward depending on the deviation of the system from equilibrium. In the case of the reaction between 70/30 cupronickel and flux 1, the transfer of metal elements might be represented by the

equations similar to Eq. 5.1:

$$Al + O \rightarrow (AlO) \qquad 5.3$$

$$Si + O \rightarrow (SiO) \qquad 5.4$$

$$Ti + Al + O \rightarrow [(TiAl)O] \qquad 5.5$$

Table 6. Chemical compositions of 70/30 cupronickel strip and claddings deposited on steel

	70Cu-30Ni Strip (wt%)	30Cu-70Ni Buttering Layer (wt%)	70Cu-30Ni 1st Layer cladding with Flux 1 (wt%)	70Cu-30Ni 1st Layer cladding with Flux 2 (wt%)
C	0.02	0.048	0.013	0.015
Mn	0.73	2.69 *	0.85	1.23
Fe	0.55	9.92 *	1.83	2.79
S	0.001	0.002	0.003	0.003
Si	0.04	0.57 *	0.15	0.29
Cu	66.99	26.19	62.26	57.63
Ni	31.25	59.31 *	34.91	37.60
Al	<0.01	0.24 *	0.030	0.12
Ti	0.42	0.89 *	0.113	0.27
Mg	<0.01	<0.001	0.001	0.007
P	0.001	0.001	<0.001	0.003
Ce	-	-	0.001	0.007
Rem	bal.	bal.	bal.	bal.

* elements tend to dilute into cupronickel cladding

According to Eq. 5.2, the reactions of 5.3 and 5.4 proceeded backward, and 5.5 could be forward, which means Al and Si decomposed from oxides and left in the weldment during melting, while Ti reacted with oxygen and transferred into the slag. These phenomena caused the weldment to decrease in Ti and increase the content of Al and Si. It explains the data shown in Table 6. Comparing the compositions between the strip and 1st layer cupronickel cladding with Flux 1, Al has been increased by 0.02%, Si has been increased by 0.11%, and Ti has been deceased by 0.3%. On the contrary, the slag has decreased Al and Si while gaining Ti and Cu elements from the alloy (Table 7).

Table 7. SEM/EDS analysis of fluxes and slags showing average trends in elemental composition

	Flux 1 (wt%)	Slag 1 (wt%)	Flux 2 (wt%)	Slag 2 (wt%)
O	10	28	15	20
F	35	5	15	5
Na	1	1	-	-
Al	8	6	10	8
Si	4	3	2	1.5
Ca	41	50	30	38
Ti	-	1.2	-	4
Mn	-	1	1	1.5
Fe	-	0.8	-	1
Ni	-	2	-	2
Cu	-	1	-	2
Ce	-	-	10	9
Zr	-	-	1	1
K	1	1	4	4
Mg	-	-	2	3

In cladding 2 (with flux 2), a more complicated reaction took place in addition to the reactions in cladding 1 due to the existence of the reactive element Ce. The transfer of metal elements between the metal and slag might be the following:

$$Al+O \rightarrow (AlO) \qquad\qquad 5.6$$

$$Si+O \rightarrow (SiO) \qquad\qquad 5.7$$

$$Ce+F \rightarrow (CeF) \qquad\qquad 5.8$$

$$Ti+Al+O \rightarrow [(Ti,Al)O] \qquad\qquad 5.9$$

$$Al+S+P+Ti+Ce+O \rightarrow [(Al,S,P,Ti,Ce)O] \qquad\qquad 5.10$$
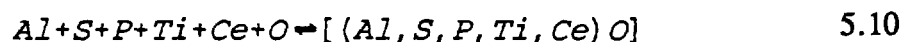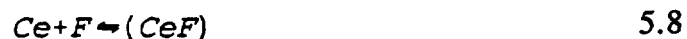
The Ce containing complex compound was a result of a slag-metalreaction. The representative X-ray spectrum of this compound is shown in Figure 16c. From the results, it is seen that this compound contains high Al, Ti, and Ce contents, and small amounts of Mg, Si, P, S, and Ca. As pointed out earlier, the oxygen which is transferred to the metal comes primarily from the decomposition of flux constituents into suboxides and oxygen. The chemical reactions would most likely take place at the slag-metal interface. Since the Ce, Al and Si are the deoxidizers, and are reported to have the capability of getting P, S, Ti etc. trace elements, they may react with oxygen and getter the trace elements to form the oxide at the slag-metal interface. The formed oxides may attach to the remaining flux thereby result in the Ce-containing complex compound. Because the density of this compound is smaller than that of the metal, most of the compounds will float up from the molten metal into the slag. Since this compound contains Ti, Mg, S etc. detrimental elements, it will bring these elements to the slag. This was the reason why much more Ti, Mg, and S were found in slag 2 than in slag 1 (Table 7). The others will remain in the molten pool and participate in the subsequent

solidification along with the molten metal. The solidification process will be discussed in detail later.

In addition to slag-metal reactions, the effect of fluxes on the compositional change of the weldment can be indirectly realized by influencing the dilution of parent metal. In the ESS process, filler metal strip is added to fusion welded cladding, and the weld deposit therefore consists of a mixture of parent metal and filler metal. When the parent metal and filler metal are dissimilar materials, the composition of weldment will be changed by the dilution of parent metal. According to Lancaster[53], dilution of parent metal is defined as

$$D = \frac{weight\ of\ parent\ metal\ melted}{total\ weight\ of\ fused\ metal} \times 100 \qquad 5.11$$

The degree of dilution is strongly related to heat input and heat input rate. As indicated by Lancaster[53], the heat input rate q is

$$q = \eta VI \qquad 5.12$$

where   V ----- voltage

I ----- current

η ----- the proportion of energy that is transferred as heat to the workpiece

the heat input (heat input rate per unit length of weld) is

$$\frac{\eta VI}{v} = \frac{q}{v} \qquad 5.13$$

where v is the welding speed. Both heat input rate and heat input will govern the dilution of parent metal, since heat input rate governs heating rate and weld pool size while heat input governs heat input amount per unit length. In this investigation, the heat input for both claddings are the same at 142kJ/in (5.6kJ/mm) while the heat input rate are 16.6kW and 22.5kW for cladding 1 and 2 respectively. Since the heat input rate of cladding 2 is higher than that of cladding 1, the dilution of parent metal is also higher. This explains

why cladding 2 contains higher concentrations of Ni, Fe, Mn, Si, Al and Ti than cladding 1 (Table 6).
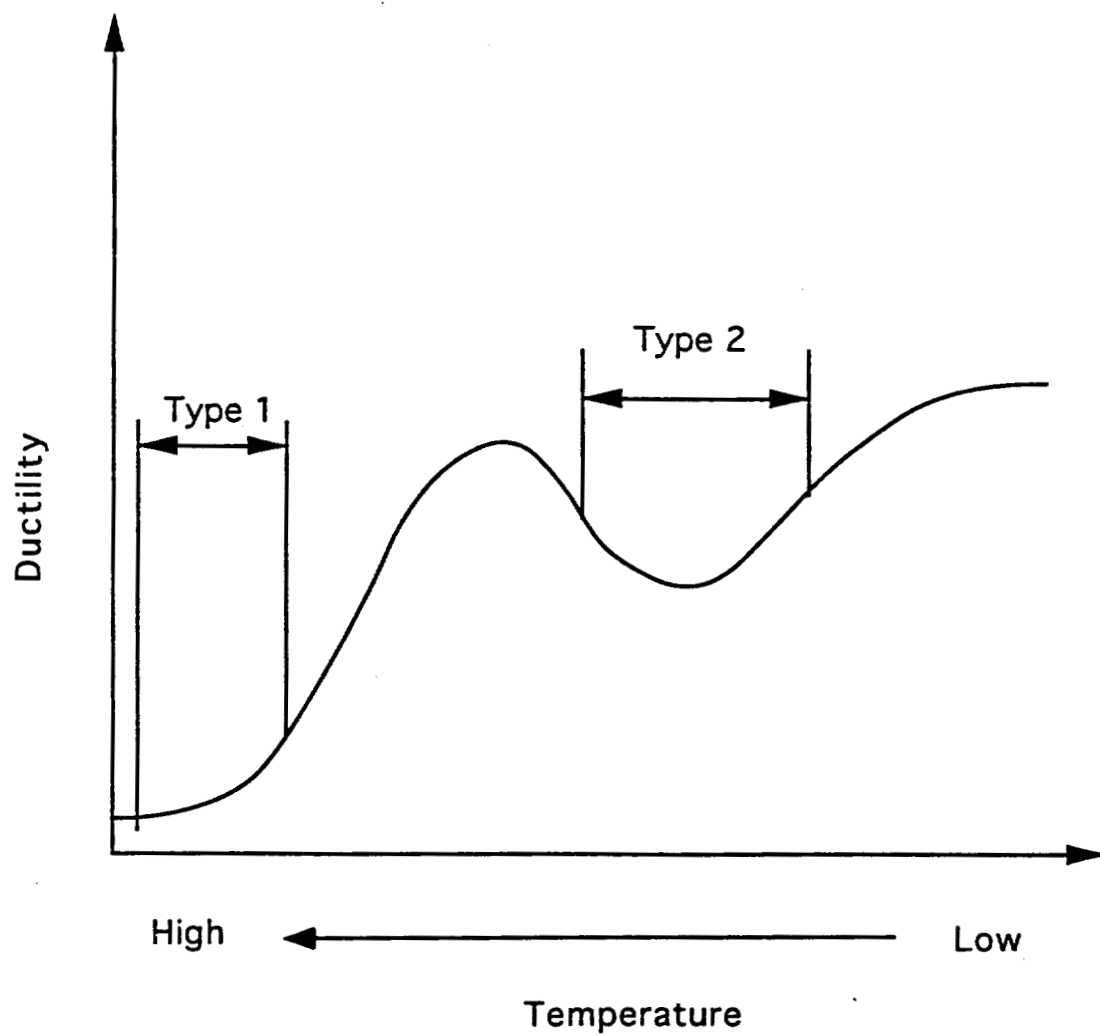
Figure 26. Schematic representation of two low-ductility temperature ranges. Type 1 occurs during solidification. Type 2 occurs immidiately after solidification.

5.2 SOLIDIFICATION CONSIDERATIONS:

When the molten metal cools, it will go through two low ductility temperature ranges during or immediately after solidification (Fig. 26). The first one takes place during solidification, and the second happens shortly after solidification. The former one will be discussed in this section, and the latter one in the next section.

In general, solidification cracking occurs when the tensile stress develops as a result of contraction exceed the corresponding fracture stress. The criteria of crack generation can be given by the equation:

$$\varepsilon \geq \delta_{min} \hspace{4cm} 5.14$$

where ε ----- strain caused by the tensile stress developed as a result of contraction (shrinkage)

δ ----- strain which the weld metal could sustain during solidification

Due to the contraction upon cooling, ε will increase with decreasing temperature. When a liquid alloy cools below its liquidus temperature, solid crystals are nucleated and grow until, at a certain temperature, they join together and form coherent bonds. At this temperature, the alloy first acquires mechanical strength. At first it is brittle, but on further cooling to the nil-ductility temperature, ductility appears and rises sharply as the temperature is reduced still further. The interval between the coherence and nil-ductility temperatures is known as the brittleness temperature range. Therefore, the ability of metal to undergo elastic and plastic deformation at high temperature without failure could be determined from the rate of increase of deformations with decrease in temperature and the ductility of the fused metal in the brittleness temperature range. As shown in schematic representation in Figure 27, the occurrence of cracking could be determined by the relationship between $\frac{\partial \varepsilon}{\partial T}$ and δ_{min}. When the rate of increase of deformation is like line 1, $\varepsilon < \delta_{min}$, cracking will not occur. When the rate of increase of deformation is like line 2, $\varepsilon = \delta_{min}$, it is the critical condition for the crack to occur. When the rate of increase of deformation is like line 3, $\varepsilon > \delta_{min}$, cracking occurs readily. So, the
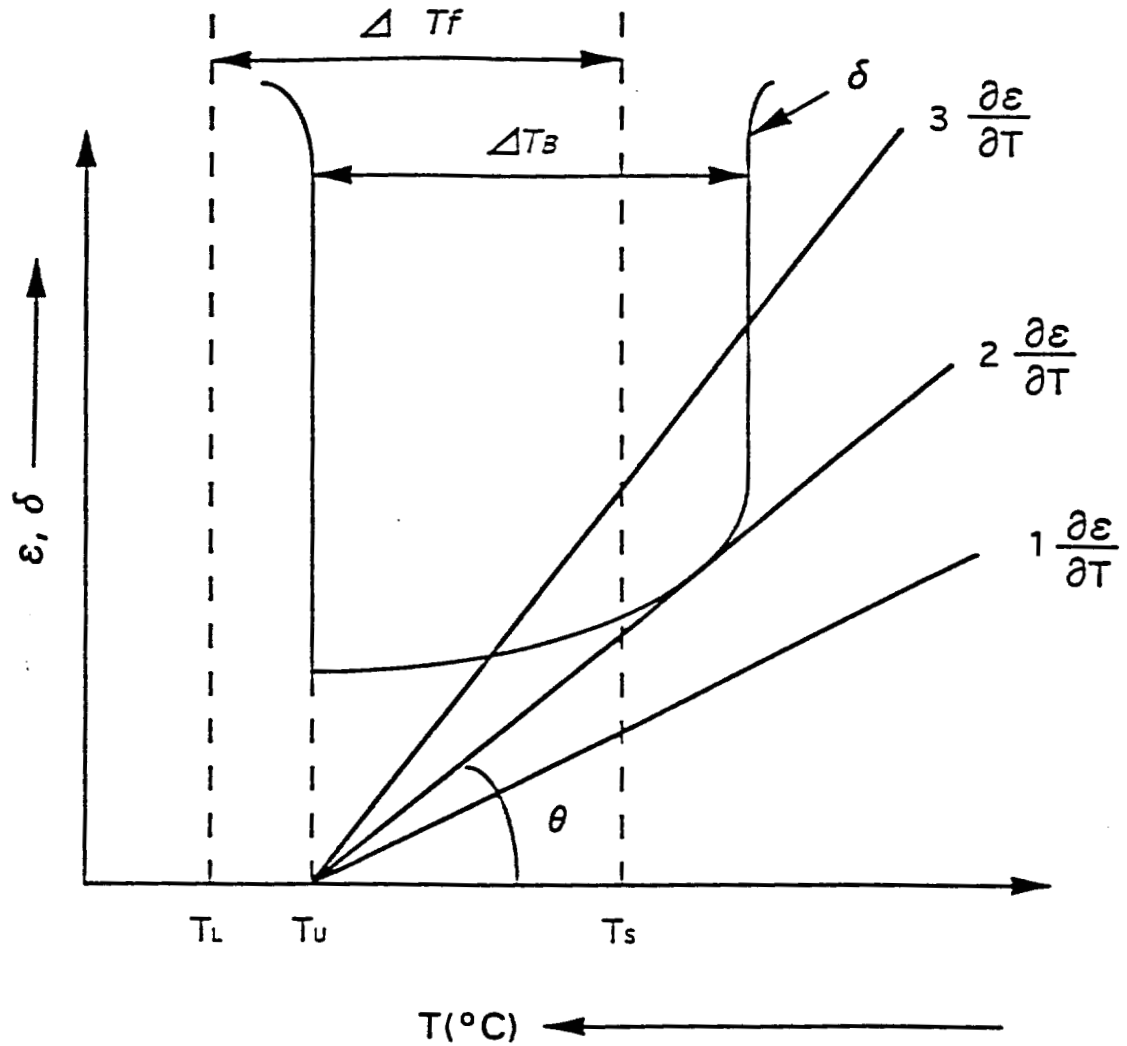
Figure 27. Solidification cracking generation diagram where:
ΔT_f--- Solidification temperature range
ΔT_B--- Brittleness temperature range
T_L--- Liquidus temperature
T_s--- Solidus temperature
δ --- Ductility curve
$\partial \varepsilon / \partial T$ --- Deformation curve

smaller the brittleness temperature range and the higher the minimum ductility, the less sensitive the alloy will be to hot cracking. In most the cases, ΔT_B and δ_{min} are influenced by the composition of the alloy, the distribution of alloy elements, the grain size and shape, and the distribution of liquid phase during dendritic solidification. The factors which influence $\frac{\partial e}{\partial T}$ are the thermal expansion coefficient of the alloy, the temperature gradient, and the geometry of the weld pool.

Since the thermal expansion coefficient of the alloy, the temperature gradient, and the geometry of the weld pool are identical in both cladding 1 and cladding 2, the factor $\frac{\partial e}{\partial T}$ should also be the same. Therefore, cladding 1, which cracked, must have a wider brittleness temperature range and lower high temperature ductility than cladding 2. How is this possible? A reexamination of the experimental results is in order. As mentioned previously, the alloy composition will influence ΔT_B and δ_{min}. Since the ratio of Cu to Ni content in cladding 2 (1.5) is less than that of cladding 1 (1.8), as a result of the buttering metal dilution (Table 6), the increasing of Ni content will narrow the brittleness temperature range and increase the minimum high temperature ductility. Therefore the weldability of the alloy will be increased.

As pointed out earlier, solidification cracking is intimately related to the segregation of alloying elements during solidification. The segregants form low melting phases or eutectics with the metal to produce highly wetting films at grain boundaries. These films weaken the structure to the extent that cracks form at the boundaries under the influence of the tensile residual stresses that occur during cooling. Impurities or alloying elements having a low equilibrium partition coefficient, k, would most likely segregate. In the case of cupronickel, any alloying constituent which exhibits a wide freezing range would have a low value of k. Some approximate values of k for alloys of copper, as determined from their binary equilibrium solubilities, are given in Table 8.

Table 8. Equilibrium partition coefficient for copper binary alloys

K_O	K_S	K_P	K_{Mg}	K_{Ti}	K_{Mn}	K_{Si}	K_{Al}	K_{Fe}
0.02	0.02	0.2	0.26	0.36	0.63	0.73	0.87	1.31

The results indicate that the elements most likely to segregate in copper base alloy are O, S, P, Mg, Ti, Mn, Si, Al, in that order. Of these elements, S, P are often considered to be the most dangerous because they could form low freezing point liquid films and brittle solid films during solidification and subsequent cooling.[5,8,13,15] In this investigation, S and P contents were controlled to be less than 0.004%wt (Table 6). The content of Mg is also low (0.01%wt). Therefore the effect of S, P and Mg can be neglected. Oxygen is another major impurity of cupronickel alloy. The presence of oxygen may result in the formation of $Cu-Cu_2O$ eutectic. This eutectic is reported[56] to be brittle. The presence of the eutectic would reduce the ductility of the alloy. However, this eutectic also has a high melting point (1066^0C), and will not significantly effect the alloy's solidification activity. Titanium, then, must be considered a key factor in generating hot cracking. It is well known that Ti is a deoxidant. Adding a small amount of it (about 0.1% wt) to the cupronickel alloy will help to reduce the gas evolution and improve weldability. However, some previous researchers[7,13,14] also indicated that if the Ti content exceeded a certain level (0.15% wt), it could cause weld metal cracking. This was associated with the formation of low freezing point eutectics which persisted in the interdendritic regions and thereby caused cracking during solidification. The phenomenon of Ti segregation has been observed in elemental distribution profile at fracture surface of cladding 1 (Fig. 25). In this profile, Ti has been observed having almost 4 times the concentration in the cracked surface than in the artificially fractured dimple area which was considered to be a non-cracking area. Compared to cladding 1, the fracture surface of cladding 2 only exhibited ductile dimple structure and the Ti was always found inside the ductile dimples in the form of inclusions. Such results indicate that Ti tends to segregate at interdendritic and grain boundary regions. When a sufficient amount of it remains in the alloy and participates in the subsequent solidification, it would lower the whole system final freezing temperature, therefore widen the brittleness temperature range and cause cracking. This is the case in cladding 1. However, when an element, such as Ce, is introduced from the flux to react with those Ti and other detrimental elements at higher temperatures, the actual amounts of detrimental elements which

participate in the subsequent solidification will be much lower and be tolerable in the alloy. Such a reaction process will efficiently prevent solidification cracking.

The image analysis and line scan profiles also provided the evidences for this hypothesis. According to the results of image analysis, cladding 2 contained 0.6% inclusions, while cladding 1 contained 0.4% which was only 2/3 amount in cladding 2. X-ray analysis showed the inclusions in cladding 2 were basically [(Al,Ti,Ce)O] type oxide, Al_2O_3, (Al,Ti)O, and SiO_2 oxides. The inclusions in cladding 1 were Al_2O_3, (Al,Ti)O and SiO_2 oxides. The higher volume fraction of precipitates in cladding 2 can be understood in two ways. One is that cladding 2 contains higher concentrations of trace elements than cladding 1 due to the higher degree of dilution. The other is that more slag-metal reactions take place in cladding 2 due to the presence of the reactive element Ce. Such reactions generate high melting point oxides and help to reduce the effect of segregating impurities in the subsequent solidification process. Moreover, the line scan profiles also confirmed this hypothesis. Looking back to Figure 17, cladding 1 has trace elements Al, Si, and Ti in high concentrations at interdendritic areas, which means a different distribution of trace elements takes place between the two claddings because of different slag-metal reactions taking place before solidification. In cladding 2, inclusions rather than trace alloying elements were generated.

In order to further verify this concept, a new flux which mixed with 90%wt flux 1 and 10%wt CeF_3 was used in depositing a new cupronickel weld. After examining the cross-sections, one was parallel to the surface, the other was perpendicular to the surface, this new weld was found free from cracking. Further investigation showed that the same kind of Ce-containing complex compound presented inside the cladding with high amounts of Ce, Al, Ti, and small amounts of Mg, Si and Ca. This experiment confirmed that Ce played an important role in eliminating cracking.

In addition to Ti, S, P, and Mg, the behavior of Fe, Si and Al in solidification activity were also studied. Since the cupronickel alloy strip was clad on the steel plate, the dilution of Fe into the weldment was inevitable. Fe is generally considered an innocuous alloying addition and having little effect on either the mechanical properties

or weldability at low concentrations in cupronickel alloys.[7,8] However, excessive iron also causes severe cracking of the weld metal and lowers the corrosion resistance of the weldment. Wilson and his co-workers[55] studied the effect of iron dilution on cupronickel weld deposits and indicated that 16% wt iron was the maximum level for 70/30 cupronickel alloy to avoid cracking, and 11.8% wt iron was the maximum level for 70/30 cupronickel alloy to avoid losing corrosion resistance. In order to reduce the effect of Fe dilution on cupronickel weldment, a buttering material, 70Ni-30Cu, was used in this study. Therefore, in the first layer of cupronickel cladding (Table 6), the Fe content in both cladding 1 and 2 were less than 3% wt. This amount was considered a safe amount for a sound weldment.

Silicon is usually considered a detrimental element in cupronickel alloys. It was reported by Billingham et al[12] that a pronounced ductility trough occurred as Si was increased to 0.5%wt. Silicon was also reported to be a weld metal crack promoter by Petersen[7] when above 0.6%wt and by Jordan[13] at the level of 1%. In this investigation, the Si constituent in cupronickel cladding was primarily introduced by fluxes, and the level of it in both cladding 1 and 2 were below 0.3% wt. Based on the data provided above, this amount is safe. Furthermore, the metallographic and fractographic examination of both claddings did not exhibit any evidence that Si could be a problem. The elemental distribution profile at fracture surface of cladding 1 (Fig. 25) and line scan profile (Fig. 17) did not show significant segregation of this element. This result was consistent with its equilibrium partition coefficient k, 0.73, which was relatively high compared to that of the other elements.

Aluminum is generally considered to be a harmless alloy addition. It is used as a deoxidizer in the cupronickel alloy to tie up nitrogen and oxygen. In this investigation, the Al constituent in both cladding 1 and 2 were below 0.2% wt. This amount would not cause any problem at all.

5.3 POST-SOLIDIFICATION CONSIDERATIONS:

As pointed in the last section, most alloys, when cooling immediately after solidification, will undergo another low ductility temperature range (Fig. 26). This low ductility temperature range is a susceptible temperature range to ductility-dip cracking. The metallographic and fractographic features of ductility-dip cracking has already been described previously. As indicated by Matsuda,[51,54] ductility-dip cracking is considered to be caused by the separation of migrated grain boundaries after solidification is completed. His experimental results indicated that when part of the grain boundary began to migrate at high temperatures, the remaining parts of the grain boundary were attached to inclusions, which were generally supposed to be part of a low melting liquid phase at that moment. He also reported that the crack traversed the cellular dendrites except for inclusions and thus mainly passed through a migrated grain boundary. Therefore, elemental segregation, precipitation, or sliding of migrated grain boundaries were considered to be the factors to cause cracking. In cladding 1, Ti, Al, Si elemental segregation has been observed (Fig. 17 and 25). Many inclusions, such as (Al,Ti)-rich inclusions and S-rich inclusions, were found lying at the cracking surfaces (Fig. 22). This segregation and precipitation may cause ductility-dip cracking in cladding 1. In cladding 2, when a reactive element Ce was introduced to the weldments, segregation has been prevented. This method which was used to avoid solidification cracking may be effective for ductility-dip cracking as well.

5.4 MULTI-LAYER CONSIDERATIONS:

Multi-layer cupronickel weld metal was found to have problems of microcracking. This problem occurred in the welds of such alloy due to the frequent development of microcracking in the weld metal of a preceding bead when this is heated by a succeeding bead. According to Lancaster,[53] when ductility-dip cracking occurred in multi-layer welding, it could occur below the finishing pass due to tensile straining in the susceptible

Table 9. Compositions of 70/30 cupronickel strip and
each layer of cladding 2

	70Cu-30Ni Strip Comp (wt%)	70Ni-30Cu Layer #1 (wt%)	70Cu-30Ni Layer #2 (wt%)	70Cu-30Ni Layer #3 (wt%)	70Cu-30Ni Layer #4 (wt%)	70Cu-30Ni Layer #5 (wt%)
C	0.02	0.048	0.015	0.008	0.007	0.006
Mn	0.73	2.69	1.23	0.83	0.71	0.69
Fe	0.55	9.92	2.79	0.95	0.53	0.48
S	0.001	0.002	0.003	0.003	0.003	0.003
Si	0.04	0.57	0.29	0.17	0.15	0.16
Cu	66.99	26.19	57.63	66.06	67.66	67.85
Ni	31.25	59.31	37.60	31.61	30.57	30.48
Cr	-	0.053	0.016	0.007	0.003	0.002
Al	<0.01	0.24	0.12	0.12	0.14	0.13
Ti	0.42	0.89	0.27	0.16	0.17	0.15
Mg	<0.01	<0.001	0.007	0.011	0.022	0.016
Co	0.01	0.013	0.007	0.004	0.004	0.005
Mo	-	0.044	0.013	0.003	<0.001	0.002
Cb	-	0.009	0.445	0.001	0.001	0.002
P	0.001	0.001	0.003	0.003	0.003	0.003
B	-	0.003	0.002	<0.001	<0.001	<0.001
Ca	-	0.001	0.003	0.002	0.004	0.003
Ce	-	0.003	0.007	0.007	0.017	0.013
V	-	0.004	-	0.001	0.001	0.002
W	-	<0.001	<0.001	0.006	0.001	0.002
Zr	-	0.001	0.003	0.001	0.001	0.001

temperature range (possibly during the heating phase of the weld thermal cycle). Figure 7 which showed a cross-section of 3 layers of cupronickel welds in cladding 1 confirmed this theory. It is obvious to see the cracking getting less and less from the 1st layer cupronickel to the last layer. The cracking underneath the surface could not be detected by surface crack detection methods, but it did show up in side bend tests. Changes in welding procedure, in this project by using a beneficial flux, could eliminate the cracks. Cladding 2 proves this concept.

In cladding of cupronickel over steel plate, the permeation of iron atoms from base metal steel into the weld metal could cause a problem. A buttering layer of nickel base alloy (70%Ni-30%Cu) has been used in this project to prevent cracking. Due to the dilution of the buttering metal, the first layer cupronickel cladding contains more Ni content than the alloy itself. Table 9 shows that only after three layers does chemical composition of the layer return back to that of the strip. In the other words, there must be three layers of weld metal deposited on steel, which are one layer of buttering material and two layers of weld metal, that can eliminate the effects of base metal and buttering metal dilution.

5.5 SUMMARY

The effect of flux on the weldability of multi-layer cladding deposited on steel with 70/30 cupronickel strip electrodes by the electroslag surfacing (ESS) process has been investigated in this research. Generally speaking, during the ESS process, the alloy composition can be changed by either slag-metal reaction or base metal dilution. Such a compositional change of the cladding results in the change of structure and quality.

When flux 1 is used, no beneficial element is introduced. Although the dilution of buttering metal is relatively low, the trace elements such as Mn, Fe, Si, Al and Ti are still diluted into the cladding along with Ni. The equilibrium partition coefficient, k, for copper binary alloys has been calculated. The element Ti has been found having a

low value of k (0.36). Moreover, the segregation of Ti has been found at both fracture surface and line scan profile in cladding 1. Based on the Cu-Ti binary phase diagram,[57] the presence of Ti in cupronickel alloy could reduce the whole system freezing temperature about 200°C (from 1084°C to 885°C). When the trace element Ti segregates to grain boundaries, it will form low freezing phases and produce highly wetting films at grain boundaries, therefore weaken the structure to the extent that cracks form at the boundaries under the influence of the tensile residual stresses that occur during cooling.

When flux 2 is used, the dilution of the buttering metal is higher than that of cladding 1. A beneficial element Ni along with other trace elements Fe, Ti, and Mn go into the 1st layer cupronickel cladding. Since the solid solubilities of elements Fe, Ti, and Mg are bigger in Ni base alloy than in Cu base alloy, the increased Ni content in cupronickel alloy will help to dissolve higher amounts of trace elements. In the other words, as the Ni content increases, the cupronickel alloy will be more tolerable to impurities. In addition, during welding, the reactive element, Ce, is introduced from the flux to react with the detrimental elements Ti, S, P, and Mg at high temperatures to reduce the level of the elements in solution, thereby reduce the degree of segregation. These reactions will efficiently prevent solidification cracking in cupronickel cladding deposited on MIL-S-23284, class 1 steel with a buttering layer of 70Ni-30Cu.

CHAPTER 6
CONCLUSIONS

The effect of flux on the weldability of multi-layer cladding deposited on steel with 70/30 cupronickel strip electrodes by the electroslag surfacing (ESS) process has been investigated. The following were the conclusions:

(1). In comparing the claddings deposited with flux 1 and 2, cladding 1 revealed severe solidification and ductility-dip cracking while cladding 2 exhibited extremely cracking resistance.

(2). The segregation of interdendritic Ti and other low melting constituents resulted in the lowering of the liquidus and solidus temperatures of the cupronickel alloy, and was responsible for cracking.

(3). The choice of flux influenced the mechanics of solidification and therefore, the form and severity of the microsegregation. Hot cracks can be prevented by using the beneficial flux (CeF_3 containing flux).

(4). The prevention of cracking was associated with the slag-metal reaction taking place in the molten pool during ESS process. When depositing with the CeF_3 containing flux, the addition of Ce reacted with Ti and other detrimental elements, such as S, P, O and Mg, to form innocuous complex Ce-containing compounds. In cupronickel cladding deposited with CeF_3 containing flux, innocuous inclusions rather than trace alloying elements were generated. As a result, the Ce provided a means to significantly eliminate cracking by mitigate the effect of detrimental trace elements responsible for solidification cracking and ductility-dip cracking.

REFERENCES

1. B.B. Moreton, "Copper Alloys in Marine Environments Today & Tomorrow", Copper Alloys in Marine Environments, Birmingham, UK, 1-2 Apr. 1985, Copper Development Association, UK, Paper No. 1.

2. M.B. Rockel, "Availability and Typical Uses of Copper Alloy Plate and Sheet", Copper Alloys in Marine Environments, Birmingham, UK, 1-2 Apr. 1985, Copper Development Association, UK, Paper No.2.

3. L.W. Sandor, "Joining Techniques for Copper-Nickel Sheathing of Offshore Structures and hips' Hulls", Copper Alloys in Marine Environments, Birmingham, UK, 1-2 Apr. 1985, Copper Development Association, UK, Paper No. 18.

4. H. Pircher and B. Ruhland, "Use of Copper-Nickel Cladding on Ship and Boat Hulls", Copper Alloys in Marine Environments, Birmingham, UK, 1-2 Apr. 1985, Copper Development Association, UK, Paper No. 5.

5. J. W. Lee, E. E. Nichols and S. Goodman, "Varestraint [Weldability} Testing of Cast 70Cu-30Ni Alloy " Weld. J., Aug. 1968, Vol. 47, pp. 371s-377s.

6. C. E. Witherell, "Some Factors Affecting the Weldability of the Cupro-Nickels", Weld. J., 1960, Vol. 39, pp. 411s-416s.

7. W. A. Petersen, "Weldability of a Chromium Strengthened Copper-Nickel Alloy", Weld. J., 1969, Vol. 48, pp. 425s-430s.

8. W. F. Savage, E. F. Nippes and J. E. Casteras, "Effect of Alloying Additions on the Weldability of 70Cu-30Ni", Weld. J., 1978, Vol. 57, pp. 375s-382s.

9. W. F. Savage, E. F. Nippes and T. W. Miller, "Microsegregation in 70Cu-30Ni Weld Metal", Weld. J., 1976, Vol 55, pp. 165s-173s.

10. W. F. Savage, E. F. Nippes and T. W. Miller, "Microsegregation in Partially Melted Regions of 70Cu-30Ni Weldments", Weld. J., 1976, Vol. 55, pp. 181s-187s.

11. P. W. Holsberg, "Weldability Studies of Modified 70-30 CuNi Alloys", Weld. J., Dec. 1970, Vol. 49, pp. 554s-558s.

12. J.P. Chubb, J. Billingham, P. Hancock, C. Dimbylow and G. Newcombe, "Effect of alloying and residual elements on strength and hot ductility of cast cupro-nickel", J. Metals., March 1978, pp. 20-25.

13. M. F. Jordan and A. Duncan, "Cracking in the Welding of Cupronickel Alloys", INCRA Project 329, Final Report, 1985.

14. C.R. Pease and T. E. Kihegren, "Welding of 90/10 Copper-Nickel alloy", Weld. J., 1954, Vol. 33, pp. 329-338.

15. S. A. Gavin, J. Billingham, J. P. Chubb, P. Hancock, "Effect of Trace Impurities on Hot Ductility of As-cast Cupronickel Alloys", Metals Technology, Nov. 1978, pp. 397-401.

16. E.W. Hartsell, JR. "Joining Copper and Copper Alloys", Weld. J., Feb. 1973, pp.88-100.

17. B.B. Moreton, "The Cladding of Steel With Copper-Nickel for Marine Industry Applications", International Copper Research Association, Inc., pp. 1-22.

18. M. Prager and E. W. Thiele, "Welding a Copper-Nickel Clad Ship --- Copper Mariner II", Weld. J., July 1979, pp. 17-24.

19. M. Prager, L.K. Keay, and E.W. Thiele, "Joining Copper and Copper-Nickel clad Steels", Weld. J., Sept. 1978, pp. 22-34.

20. E.A. Taylor and A.H. Burn, "Inert Gas Arc Welding of Copper and Its Alloys", Proceedings of the Commonwealth Welding Conference, 1966, pp. 224-229.

21. L. C. Minard, T. J. Kelly and N. Kenyon, "Welding of Cu-Ni Clad Steel for Hull Plate", Weld. J., May 1979, pp. 39-46.

22. "Electroslag Welding", ed. by B.E. Paton, Mir Publisher, 1980, pp. 11-18.

23. W.P. Benter, Jr. and C. G. Schilling, "Acceptance Criteria for Electroslag Weldments in Bridges", NCHRP Report 201, May 1979, pp. 3-4.

24. Y.K. Oh, J.H.Devletian and S.J. Chen, "Low Dilution Electroslag Cladding for Shipbuilding", Weld. J., Aug. 1990, Vol. 69, pp. 37-44.

25. Y.K. Oh, J.H. Devletian, "Electroslag Surfacing for Shipbuilding and Repair", Sea Technology, June 1990, pp. 46-47.

26. A. Van Bemst and Ph. Dargent, "Electroslag Cladding Using Nickel Base Alloys", Metal construction, Dec. 1983, pp. 730-733.

27. U. Heubner, T. Hoffmann and G. Rudolph, "Overlay Welding of Corrosion Resistant Nickel Superalloys", in "Weldability of Materials", R.A.Patterson and K. W. Mahin (Eds.), ASM International, Materials Park, OH, 1990, pp. 175-182.

28. Y. P. Gao, J. H. Devletian and W. E. Wood, "Electroslag and Submerged Arc Cladding with Nickel Alloy Strip", Proceeding of 3rd International Conference on Trends in Welding Research, ASM International, Gatlinburg, TN, USA, June 1-5, 1992.

29 G. R. Belton, T. J. Moore and E. S. Tankins, "Slag-Metal Reactions in Submerged Arc Welding", Weld. J., July 1963, Vol. 47, pp. 289s-297s.

30. J. H. Palm, "How Fluxes Determine Properties of SA Welds", Weld. J., July 1972, Vol. 51, pp. 358s-360s.

31. T. Lau, G.C. Weatherly and A. McLean, "The Sources of Oxygen and Nitrogen Contamination in Submerged Arc Welding Using $CaO-Al_2O_3$ Based Fluxes", Weld. J., Dec. 1985, Vol. 64, pp. 343s-347s.

32. B. M. Patchett and D.R. Milner, "Slag-Metal Reactions in the Electroslag Process", Weld. J., Oct. 1972, pp. 491s-504s.

33 U. Mitra and T.W. Eagar, "Slag-Metal Reactions during Welding: Part I. Evaluation and Reassessment of Existing Theories", Metall. Trans. B., Feb. 1991, Vol. 22B, pp. 65-71.

34. U. Mitra and T. W. Eagar, "Slag-Metal Reactions during Welding: Part II. Theory", Metall. Trans. B., Feb. 1991, Vol. 22B, pp. 73-81.

35. U. Mitra and T. W. Eagar, "Slag-Metal Reactions during Welding: Part III. Verification of the Theory", Metall. Trans. B., Feb. 1991, Vol. 22B, pp. 83-100.

36. C. S. Chai and T. W. Eagar, "Slag Metal Reactions in Binary CaF_2-Metal Oxide Welding Fluxes", Weld. J., July 1982, Vol. 61, pp. 229s-232s.

37. T. W. Eagar, "Sources of Weld Metal Oxygen Contamination During Submerged Arc Welding", Weld. J., March 1978, Vol. 57, pp. 76s-80s.

38. C. S. Chai and T. W. Eagar, "The Effect of SAW Parameters on Weld Metal Chemistry", Weld. J., March 1980, Vol. 59, pp. 93s-98s.

39. C. S. Chai and T. W. Eagar, "Slag-Metal Equilibrium During Submerged Arc Welding", Metall. Trans. B, 1981, Vol. 12B, pp. 539-547.

40. K. Easterling, "Introduction to the Physical Metallurgy of Welding", Butterworths, Hememann, 2nd Edition, 1993, 270 pp.

41. M. C. Flemings, "Solidification Processing", McGraw-Hill, New York, NY, 1974, 364 pp.

42. B. Hemsworth, T. Boniszewski, and N. F. Eaton, "Classification and Definition of High Temperature Weld Cracks in Alloys", Metal Construction, Feb. 1969, pp. 5-16.

43. N. N. Prokhorov, N. Nikol Prokhorov and M. N. Gavrilyuk, "Strain Behavior of Metals during Solidification after welding", Welding Production, Vol. 18, 1971, pp. 5-9.

44. H. F. Bishop, C. E. Ackerlind and W. S. Pellini, "Metallurgy and Mechanics of Hot Tearing", Trans. Amer. foundryman's Society 1952, Vol. 60, pp. 818.

45. W. Rostoker, J. M. McCaughey and H. Markus, "Embrittlement by Liquid Metals", New York, Reinhold, Publishing Corporation, 1960.

46. J. C. Borland, "Fundamentals of Solidification Cracking in Welds. Part I", Welding and Metal Fabrication, Jan./Feb. 1979, pp. 19-29.

47. J. C. Borland, "Fundamentals of Solidification Cracking in Welds. Part II", Welding and Metal Fabrication, Mar. 1979, pp. 99-107.

48. B. I. Medovar, "On the Nature of Weld Hot Cracking", Automatic Welding, July 1954, pp. 12-18.

49. N. N. Prokhorov, "Problems of the Strength of Metals in the Process of Solidification during Welding", Welding Production, June 1956, pp. 5-11.

50. J. A. Williams and A. R. E. Singer, "Deformation, Strength and Fracture above the Solidus Temperature", Journal of the Institute of Metals, Vol. 96, 1968, pp. 5-12.

51. F. Matsuda, H. Nakagawa, S. Ogata and S. Katayama, "Fractographic Investigation on Solidification Crack in the Varestraint Test of Fully Austenitic Stainless Steel", Transactions of JWRI, Vol. 7, No. 1, June 1978, pp. 59-70.

52. C. Z. Wu, J. Q. Liu and W. T. Ye, "On the Weldability of Cu-Alloy Cladded Steel Plate", IIW Asian Pacific Regional Welding Congress and 36th Annual AWI Conference, Hobart, P. R. China, 14-18 Nov. 1988, pp. 327-337.

53 J.F. Lancaster, "Metallurgy of Welding", Chapman & Hall, 5th Edition, New York, 1993, 389pp.

54. F. Matsuda and H. Nakagawa, "Some Fractographic Features of Various Weld Cracking and Fracture Surfaces with Scanning Electron Microscope", Transactions of JWRI, Vol. 6 No. 1, 1977, pp. 81-90.

55. R. K. Wilson, T. J. Kelly and S. D. Kiser, "The Effect of Iron Dilution on Cu-Ni Weld Deposits Used in Seawater", Weld. J., Sept. 1987, pp. 280s-287s.

56. V. K. Lebedev, V. G. Chaika, and V. A. Anoshin, "Ductile Properties of Copper Wire Joints Produced by Resistance Welding", Avtom. Svarka, 1988, Vol. 4, pp. 14-18.

57. T. B. Massalski, "Binary Alloy Phase Diagrams", 2nd Edition, ASM International, 1990.

58. T. Kobayashi, T. Kuwana, M. Ando and I. Fujita, Trans. Jap. Weld. Soc., 1970a, Vol. 1, pp. 1-11.

59. J. P. Chubb, and J. Billingham, "Effect of Nickel on Hot Ductility of Binary Copper-Nickel Alloys", Metals Technol., March 1978, Vol. 5(3), pp. 100-103.

VITA

The author was born on January 22, 1966 in Shanghai, China. She received her BS degree in Materials Science & Engineering from Shanghai Jiao Tong University, Shanghai, China in 1988. She had then worked with China New Technology Corp., Shanghai Branch for three years. In fall 1991, she joined the Materials Science Department at the Oregon Graduate Institute of Science & Technology, Beaverton, Oregon, U.S.A. where she completed the requirements for the degree Master of Science in June 1994.